Original Paper

Copper isotope fractionation between aqueous compounds relevant to low temperature geochemistry and biology

Toshiyuki Fujii[1]*, Frédéric Moynier[2], Minori Abe[3],
Keisuke Nemoto[3], and Francis Albarède[4]

[1] Research Reactor Institute, Kyoto University, 2-1010 Asashiro Nishi, Kumatori, Sennan, Osaka 590-0494, Japan

[2] Department of Earth and Planetary Sciences and McDonnell Center for Space Sciences, Washington University in St. Louis, Campus Box 1169, 1 Brookings Drive, Saint Louis, MO 63130-4862, USA

[3] Department of Chemistry, Graduate School of Science and Engineering, Tokyo Metropolitan University, 1-1 Minami-Osawa, Hachioji-shi, Tokyo 192-0397, Japan

[4] Ecole Normale Supérieure de Lyon, Université de Lyon 1, CNRS, 46, Allee d'Italie, 69364 Lyon Cedex 7, France

*Author to whom correspondence should be addressed

tosiyuki@rri.kyoto-u.ac.jp

TEL: +81-72-451-2469, FAX: +81-72-451-2634

Abstract:

Isotope fractionation between the common Cu species present in solution (Cu^{+}, Cu^{2+}, hydroxide, chloride, sulfide, carbonate, oxalate, and ascorbate) has been investigated using both *ab initio* methods and experimental solvent extraction techniques. In order to establish unambiguously the existence of equilibrium isotope fractionation (as opposed to kinetic isotope fractionation), we first performed laboratory-scale liquid-liquid distribution experiments. Upon exchange between HCl medium and a macrocyclic complex, the $^{65}Cu/^{63}Cu$ ratio fractionated by –1.06 to –0.39‰. The acidity dependence of the fractionation was appropriately explained by ligand exchange reactions between hydrated H_2O and Cl^{-} via intramolecular vibrations. The magnitude of the Cu isotope fractionation among important Cu ligands was also estimated by *ab initio* methods. The magnitude of the nuclear field shift effect to the Cu isotope fractionation represents only ~3% of the mass-dependent fractionation. The theoretical estimation was expanded to chlorides, hydroxides, sulfides, sulfates, and carbonates under different conditions of pH. Copper isotope fractionation of up to 2‰ is expected for different forms of Cu present in seawater and for different sediments (carbonates, hydroxides, and sulfides). We found that Cu in dissolved carbonates and sulfates is isotopically much heavier (+0.6‰) than free Cu. Isotope fractionation of Cu in hydroxide is minimal. The relevance of these new results to the understanding of metabolic processes was also discussed. Copper is an essential element used by a large number of proteins for electron transfer. Further theoretical estimates of $\delta^{65}Cu$ in hydrated Cu(I) and Cu(II) ions, Cu(II) ascorbates, and Cu(II) oxalate predict Cu isotope fractionation during the breakdown of ascorbate into oxalate and account for the isotopically heavy Cu found in animal kidneys.

Keywords: Copper, Cupric, isotope fractionation, ligand, quantum chemical calculation

1. INTRODUCTION

Copper has two stable isotopes, ^{63}Cu and ^{65}Cu, with respective average abundances of 69.174% and 30.826% in the reference metal SRM-NIST 976 (Shields et al., 1964). Variations of Cu isotope abundances in natural samples were identified by Walker et al. (1958) using thermal ionization mass spectrometry, but the variability of the mass bias at that time was too large with respect to the natural isotopic availability to qualify Cu isotopes as a potential geochemical or biochemical tracer. The advent of inductively-coupled plasma mass spectrometry (ICP-MS) instruments equipped with a magnetic sector and multiple collection made precise isotopic analysis of Cu possible (Albarède, 2004). Maréchal et al. (1999) published the first measurements of Cu isotope compositions in a variety of minerals and biological materials. The broad range of isotopic variations in Cu ores observed previously (Walker et al. 1958; Shields et al., 1965) was confirmed by subsequent work (Maréchal et al., 1999; Zhu et al., 2000; Albarède, 2004; Klein et al., 2009). Hereafter, the δ notation with

$$\delta^{65}Cu = \left(\frac{([^{65}Cu]/[^{63}Cu])_{sample}}{([^{65}Cu]/[^{63}Cu])_{reference}} - 1 \right) \times 1000 \quad (1)$$

is used throughout.

The narrow range of Cu isotope variation in basalts (Ben Othman et al., 2006; Archer and Vance, 2004; Herzog et al., 2009; Li et al., 2009; Moynier et al., 2010; Bishop et al., 2012) and granites (Li et al., 2009) suggests that high-temperature magmatic processes do not induce large Cu isotope fractionation. As a consequence, it makes Cu isotopes a tracer of choice for the study of sediments and more generally for

73 low-temperature processes such as those involved in soil formation (Bigalke et al., 2010,
74 2011) and in biology (Balter and Zarro, 2011; Weinstein et al., 2011).

75 Substantial isotope fractionation during chemical exchange reactions occurs at
76 room temperature and reflects isotopic differences between the equilibrium constants of
77 Cu isotopologues. Enrichment in ^{65}Cu of up to 0.8‰ was observed during the
78 chromatographic elution of compounds (Matin et al., 1998; Maréchal et al., 1999, 2002;
79 Zhu et al., 2002). The same technique demonstrates isotope fractionation of ~0.4‰
80 upon chromatographic separation of Cu(I) from Cu(II) (Matin et al., 1998; Zhu et al.,
81 2002).

82 At low temperature, Cu isotopic abundances are also affected by inorganic
83 surface processes (physical adsorption/desorption). Isotope separation of up to a few
84 permil upon adsorption/desorption of Cu onto/from inorganic and organic substrates
85 was observed by several groups (Mathur et al., 2005; Balistrieri et al., 2008; Pokrovsky
86 et al., 2008; Navarette et al., 2011).

87 Copper plays very important roles in biology (Lippard and Berg, 1994). The
88 metal centers of the 'blue' copper proteins are divided according to the coordination of
89 the Cu ion into three types that contain one or more copper ions as prosthetic groups
90 (Cowan, 1997). In plastocyanine, cysteine, histidine, and methionine 'residues' bind to
91 Cu and this plays a major role for electron transfer (redox reactions) (Freeman and Guss,
92 2001). In humans, ceruloplasmin is a ferroxidase enzyme involved in the iron cycle,
93 cytochrome c oxidase is involved in electron transfer across the membrane of
94 mitochondrion, and superoxide dismutase protects cells against superoxide. Blue (Cu)
95 proteins are ubiquitous and characterized by their multiple ways of bonding with amino
96 acids. (Cowan, 1997). Coupling of Fe and Cu isotope fractionation has been identified

97 in human blood components (Albarède et al., 2011a) and in mammals (Balter and Zazzo,
98 2011; Albarede et al., 2011b). Depletion of δ^{65}Cu at the permil level was found in plants
99 with respect to soils or nutrient solutions (Weinstein et al., 2011; Jouvin et al., 2012).
100 δ^{65}Cu in enzymes is a few permil negative compared with the Cu isotopic composition
101 of the host soil (Zhu et al., 2002). Positive δ^{65}Cu values up to 1.5‰ also were found in
102 the kidneys of sheep (Balter and Zazzo, 2011) and mice (Albarede et al., 2011b).
103 Contrary to Fe (Hill et al., 2010; Rustad et al., 2010, and references therein), Ni
104 (Fujii et al., 2011a), and Zn (Fujii et al, 2010,2011b; Black et al., 2011; Pons et al.,
105 2011; Fujii and Albarède, 2012), the theoretical prediction of Cu isotope fractionation
106 among ligands (simple inorganic ligands like halide, sulfate, and phosphate ions, and
107 more complex organic ligands as humic acids and phytoplankton exometabolites) in
108 natural waters and biological fluids has only received minimal attention, which is a
109 major hindrance for an informed interpretation of observations. This is the main
110 motivation for the present work.
111 We first demonstrate that equilibrium isotope fractionation of Cu(II) does take
112 place in laboratory-scale experiments. In parallel, we calculated the molecular orbitals
113 of the corresponding Cu species to obtain the reduced partition function ratio (RPFR) of
114 isotopologues. The *ab initio* calculations were then extended to hydrated Cu(II)
115 complexes, hydroxide, sulfate, carbonate, ascorbate, and oxalate. The choice of
116 ascorbate and oxalate was motivated by evidence of isotopically heavy Cu in the
117 kidneys of sheep (Balter and Zazzo, 2011) and mice (Albarède et al., 2011b). Ascorbate
118 is allegedly catabolized into oxalic acid (Chai et al., 2004; Massey et al., 2005;
119 González et al., 2005), which makes some patients develop a condition known as
120 hyperoxaluria and develop kidney stones, a calcium oxalate. The oxalate anions are

known to be strong complexing ligands of Cu(II) (Hayakawa et al., 1973), while ascorbate oxidase, which oxidizes ascorbate into dehydroascorbate (Solomon et al., 1996) is a bis(histidine)copper(II) compound. Applications of our calculations to the understanding of Cu isotope variability in marine sediments and to biological samples are briefly outlined.

2. METHODS

2.1. Extraction experiments and isotopic analyses

Dicyclohexano-18-crown-6 (DC18C6) (>97% purity) is a product of Fluka Chemie GmbH and Cu dichloride (hydrated, 99.9% purity) is a product of Wako Pure Chemical Industries, Ltd. Hydrochloric acid, in which the Cu impurity was certified to be less than 1.9 ppt, was purchased from Kanto Chemical, Co., Inc. Other chemicals were reagent grade.

$CuCl_2 \cdot 2H_2O$ was dissolved in HCl to prepare solutions of 0.1 mol dm^{-3} (M) Cu(II) in 1 to 6 M HCl. DC18C6 was dissolved in 1,2-dichloroethane to prepare a solution of 0.1 M DC18C6. Ten mL aqueous solution were combined with 15 mL organic solution in a glass vial, which was sealed. The two phases were stirred for 30 minutes using a Teflon-coated magnetic bar. After equilibrium was achieved, the two phases were separated by centrifugation at 2,000 rpm for 1 min, and an aliquot of the aqueous solution taken for analysis. A 10 mL aliquot of the organic solution was saved for back extraction of Cu in 15 mL of 0.02 M HCl. The extracted Cu was fully (>98%) recovered in this procedure. All these steps were carried out at 298 K. Copper concentrations in the equilibrated aqueous phase and the back extraction solution were determined by inductively-coupled plasma atomic-emission spectrometry (Thermo

145 Fisher Scientific, iCAP 6300 Duo). Aliquots of these solutions were saved for isotopic
146 analysis.

147 Organic impurities carried over from the extraction step were separated from
148 Cu on AGMP1 anion exchange resin in 7 M HCl as described in Maréchal et al. (1999).
149 Copper isotopic compositions were measured on a Thermo-Finnigan Neptune
150 MC-ICP-MS at Washington University in St. Louis. The samples were introduced by
151 free aspiration in 0.1 M HNO_3 using a Teflon microcentric nebulizer (uptake rate of 100
152 μL/min) and a glass cyclonic spray chamber. Masses 63 and 65 were positioned on the
153 L2 and axial collectors, respectively. Intensities of Zn isotopes (64, 66, 67 and 68) were
154 measured on the collectors L1, H1, H2, H3, respectively. The intensity of ^{62}Ni was
155 monitored in order to correct for the potential interference of ^{64}Ni. Instrumental mass
156 fractionation was corrected by both Zn doping and standard-sample bracketing
157 (Maréchal et al., 1999; Albarède, 2004). The typical external reproducibility of replicate
158 analyses of the same samples carried out during different analytical sessions is 0.10‰
159 (2σ) for $\delta^{65}Cu$.

160

161 **2.2. Computational methods**

162 Orbital geometries and vibrational frequencies of aqueous Cu(II) species were
163 computed using the density functional theory (DFT) as implemented by the Gaussian09
164 code (Frisch et al., 2009; Dannington et al., 2009). The DFT method employed here is a
165 hybrid density functional consisting of Becke's three-parameter non-local hybrid
166 exchange potential (B3) (Becke, 1993) with Lee-Yang-and Parr (LYP) (Lee et al., 1988)
167 non-local functionals. Using the 6-311+G(d,p) basis set or higher is recommended for
168 calculating the Cu complexes by de Bruin et al. (1999). The 6-311+G(d,p) basis set,

which is an all-electron basis set, was therefore chosen for H, C, O, S, Cl, and Cu. Molecules were modeled without any forced symmetry. An 'ultrafine' numerical integration grid was used and the SCF (self-consistent field) convergence criterion was set to 10^{-9}.

The isotope enrichment factor due to intramolecular vibrations can then be evaluated from the reduced partition function ratio (*s*/*s*')*f* (Bigeleisen and Mayer, 1947), also noted β,

$$ln\frac{s}{s'}f = \sum\left[ln\,b(u_i') - ln\,b(u_i)\right] \tag{2}$$

where

$$ln\,b(u_i) = -ln\,u_i + \frac{u_i}{2} + ln\left(1 - e^{-u_i}\right) \tag{3}$$

and

$$u_i = \frac{h\nu_i}{kT} \tag{4}$$

in which ν stands for vibrational frequency, *s* for the symmetry number of the Cu compound, *h* the Planck constant, *k* the Boltzmann constant, and *T* the absolute temperature. The subscript *i* denotes the *i*th mode of molecular vibration, and primed variables refer to the light isotopologue. The isotope enrichment factor due to molecular vibrations can be evaluated from the frequencies (ν) summed over all the different modes. The isotopic difference in the stability constant of chemical reactions is identical to the difference of ln β between related species. For example, a chemical exchange reaction,

$$Cu^{2+} + Cl^- \rightleftarrows CuCl^+, \quad K_{CuCl^+} \tag{5}$$

187

188 with stability constant K_{CuCl^+}, the isotope fractionation between the hydrated Cu^{2+} and

189 $CuCl^+$ is,

$$\ln \frac{K_{CuCl^+}(^{65}Cu)}{K_{CuCl^+}(^{63}Cu)} = \ln \frac{[^{65}CuCl^+]/[^{63}CuCl^+]}{[^{65}Cu^{2+}]/[^{63}Cu^{2+}]}$$

190

$$= \ln \beta_{CuCl^+} - \ln \beta_{Cu^{2+}} \quad (6)$$

191

192 Isotope fractionation also results from the mass-independent nuclear field shift

193 effect (Bigeleisen, 1996; Nomura et al., 1996, Fujii et al. 2009) which is an

194 isotope-dependent shift reflecting that the electronic orbitals do not vanish at the

195 nucleus and depends on the nuclear size and shape (King, 1984). The latest version of

196 quantum chemical models have taken finite-size nuclei into account in *ab initio*

197 calculations (Schauble, 2007; Abe et al., 2008, 2010; Fujii et al., 2010, 2011a,c,d). For

198 light elements such as Ni (Fujii et al., 2011a) and Zn (Fujii et al., 2010), the nuclear

199 field shift effect was found to be small as 0.02-0.03‰/amu. The isotope enrichment

200 factor via the nuclear field shift ($\ln K_{fs}$) is given by

201

$$\ln K_{fs} = \frac{hc}{kT} \nu_{fs} \quad (7)$$

202

203 where ν_{fs} is the nuclear field shift and c the velocity of light.

204 The contribution of the nuclear volume was estimated by the Dirac-Coulomb

205 Hartree-Fock (DCHF) method implemented in the UTChem program (see references in

206 Abe et al., 2008, 2010). We calculated the electronic structure of Cu^0([Ar]3d^{10}4s^1),
207 Cu^+([Ar]3d^{10}), Cu^{2+}([Ar]3d^9) and a few other simple Cu molecules. The Cartesian
208 coordinates of Cu molecules optimized by the Gaussian09 code were supplied to the
209 DCHF calculation. Exponents of basis sets were taken from Faegri's four-component
210 basis for Cu (Faegri, 2001), third-order Douglas-Kroll basis for H and Cl (Tsuchiya et
211 al., 2001), and ANO-RCC for O (Roos et al., 2005). Contraction coefficients were
212 optimized by four-component atomic calculations (Koc and Ishikawa, 1994). After
213 adding some diffuse and polarization functions, the final contraction form of the large
214 component basis sets was (19*s*14*p*9*d*)/[6*s*4*p*3*d*] for Cu, (16*s*11*p*1*d*)/[4*s*3*p*1*d*] for Cl,
215 (14*s*9*p*2*d*)/[3*s*2*p*2*d*] for O, and (8*s*2*p*)/[3*s*2*p*] for H.

216 The effect of nuclear spin can be neglected at equilibrium (Bigeleisen, 1996).
217 Since the present crown ether experiments were run at equilibrium, the kinetic part of
218 this effect also known as the magnetic isotope effect (Epov et al., 2011; Epov, 2011),
219 will not be considered in this work.

220

221 ## 3. RESULTS AND DISCUSSION

222 ### 3.1. Isotope fractionation of Cu by crown ether extraction

223 The Cu(II) species in HCl medium in the laboratory experiment are Cu^{2+},
224 $CuCl^+$, $CuCl_2$, and $CuCl_3^-$ (Brugger et al., 2001), which are related through
225 complexation reaction 5 and the following stepwise reactions, with stability constants
226 K_{species},

$$CuCl^+ + Cl^- \rightleftarrows CuCl_2, \quad K_{CuCl_2} \tag{8}$$

227 and

$$CuCl_2 + Cl^- \rightleftarrows CuCl_3^-, \quad K_{CuCl_3^-} \tag{9}$$

228

229 The presence of $CuCl_4^{2-}$ was reported for highly concentrated HCl and $CuCl_2$ systems
230 (Bell et al., 1973; Neilson, 1982; Tanimizu et al., 2007) or high-temperature systems
231 (Collings et al., 2000) but this higher order of complexation is negligible at the low HCl
232 concentrations and ambient temperature of the present experiments (Brugger et al.,
233 2001).

234 The extraction reaction of Cu(II) with the macrocyclic ligand can be written as,

$$CuCl_2 + L \rightleftarrows CuLCl_2, \tag{10}$$

235

236 where L stands for DC18C6. The distribution ratio *D* is written as,

$$D = \frac{\Sigma[\mathrm{Cu(II)}]_{org}}{\Sigma[\mathrm{Cu(II)}]_{aq}} \approx \frac{[CuLCl_2]}{[Cu^{2+}] + [CuCl^+] + [CuCl_2] + [CuCl_3^-]} \tag{11}$$

237

238 where the subscripts 'org' and 'aq' stand for the organic and aqueous phases,
239 respectively.

240 The isotope separation factor α, between the aqueous and organic phases, is
241 defined as:

$$\alpha = \frac{\sum_k \varphi_{org}^k \left({}^{65}Cu/{}^{63}Cu\right)_{org}^k}{\sum_k \varphi_{aq}^k \left({}^{65}Cu/{}^{63}Cu\right)_{aq}^k} \tag{12}$$

242

where *k* refers to the *k*th compound in the organic and aqueous phases, respectively, and φ is the fraction of total Cu (proper ^{63}Cu) hosted in the *k*th compound. The isotope enrichment factor is defined as $\alpha - 1$. Because α is always close to unity, $\alpha - 1 \approx \ln \alpha$, and 1000 ln α therefore can be approximated by $\Delta^{65}Cu = \delta^{65}Cu_{org} - \delta^{65}Cu_{aq}$. The $\Delta^{65}Cu$ values obtained are shown in Table 1 together with distribution ratios. $\Delta^{65}Cu$ ranged from –1.06 to –0.39‰.

The yield of Cu(II) extraction by crown ethers has been investigated by Yoshio et al. (1980), Nakamura et al. (1982), and Contreras et al. (1993). A study on extraction kinetics showed that equilibrium is achieved within 30 sec (Nakamura et al., 1982). Hydration-dehydration is known to be the rate-limiting step of solvent extraction. The rate constant for H_2O substitution in the inner coordination sphere of Cu^{2+} is quite high in the transition metal series, and it is comparable with that of Li^+ of the alkali metals as observed by Eigen (1963). The isotope exchange rate kinetics of $^7Li/^6Li$ in the crown ether systems has been studied in detail (Jepson and Cairns, 1979; Nishizawa et al., 1984), in which the isotopic equilibrium is achieved within 30-60 sec after contacting aqueous and organic phases. The 30 min stirring period in the present study is therefore considered to be enough to achieve the isotopic equilibrium of Cu. The $\Delta^{65}Cu$ values listed in Table 1 are hence attributable to the equilibrium isotope effect.

Figure 1a shows the mole fractions of Cu species estimated by using the stability constants of reactions 5, 8, and 9 (Brugger et al., 2001). $\Delta^{65}Cu$ was found to vary with HCl molarity (Fig. 1b), a trend that reflects the isotope fractionation of Cu in reactions 5 and 8-10. With increasing HCl molarity, more $CuCl_2$ forms, which in turn results in an increase of *D*. The magnitude of $\Delta^{65}Cu$ shown in Table 1 is similar to that

found in other ligand exchange systems (Matin et al., 1998; Maréchal et al., 1999, 2002; Zhu et al., 2002).

3.2. Contribution of the mass-independent isotope effect

The total electronic energies calculated for Cu isotopes and isotopologues are shown in atomic units (a.u.) in Table 2, in which Cu^{2+} was chosen as the reference. The maximum effect was found to be 0.015‰ for the Cu^0-Cu(I) pair and 0.012‰ for the Cu(I)-Cu(II) pair. The solvent extraction reaction is controlled by ligand exchange of Cu(II). Based on the Cu(II) data in Table 2, the nuclear field shift effect in Cu(II) species is only ~3% of the smallest Δ^{65}Cu value listed in Table 1. The values of Δ^{65}Cu reported in Table 1 are the values for the mass-dependent isotope fractionation and reflect intramolecular vibrations.

3.3. Mass-dependent isotope effects

3.3.1. Hydrated Cu(II) ions

The hydrated Cu(II) ion is generally represented as the hexaaqua complex $Cu(H_2O)_6^{2+}$ (Fig. 2). It is known that $Cu(H_2O)_6^{2+}$ shows the Jahn-Teller distortion effect (Sherman, 2001; Bersuker, 2006). Two Cu-O distances of the vertical axial bond ($Cu\text{-}O_{ax}$) are longer than four Cu-O distances in the equatorial plane ($Cu\text{-}O_{eq}$). The Jahn-Teller effect lowers the symmetry of $Cu(H_2O)_6^{2+}$ from octahedral T_h to D_{2h}. The calculated bond distance of Cu-O and the literature values are shown in Table 3. The bond distances were calculated to be 2.02-2.03 Å ($Cu\text{-}O_{eq}$) and 2.30 Å ($Cu\text{-}O_{ax}$), which are consistent with those reported in the literature (see references in Table 3).

289 After evidence was found that the stable aqueous complex has a fivefold
290 coordination (Pasquarello et al., 2001), the Jahn-Taller effect of $Cu(H_2O)_6^{2+}$ in aqueous
291 solutions has been questioned (Chaboy et al., 2006). The $Cu(H_2O)_5^{2+}$ complex has five
292 identical Cu-O bonds with a length of 1.96 Å, which was identified by neutron
293 diffraction (ND) analysis combined with first-principles molecular dynamics (MD). The
294 common bond distance reflects the rapid switch between the square pyramid and
295 trigonal bipyramid configurations (Pasquarello et al., 2001; de Almeida et al., 2008). In
296 a Car-Parrinello MD simulation (Amira et al., 2005), a square pyramidal geometry with
297 four short (2.00 Å) and one long (2.45 Å) Cu-O bond could be optimized. A similar set
298 of bond distances, four short (1.97 Å) and one long (2.39 Å) Cu-O bond, has been
299 confirmed in an X-ray absorption study (Benfatto et al., 2002). Our calculation of the
300 $Cu(H_2O)_5^{2+}$ geometry also resulted in the square pyramid rather than the trigonal
301 bipyramid of Fig. 2 and Table 4.
302 There is no clearly predominant structure among the four-, five-, and six- fold
303 coordinated Cu(II) ions (Chaboy et al., 2006). In the present study, we tested both the
304 coordination numbers five and six. We also tested a coordination number four to
305 evaluate the possibility of steric hindrance and strong degree of covalency. The
306 optimized structures in Cartesian coordinates are given in Table S1 of the electronic
307 supplement.
308 The intramolecular vibrational frequencies were then calculated for aqueous
309 Cu(II) species with optimized geometries. The ln β [= ln (*s*/*s*')*f*] values for the isotope
310 pair $^{65}Cu/^{63}Cu$ were determined by employing Eqs. 2-4 and are listed in Table 5. The
311 value of ln β of $Cu(H_2O)_5^{2+}$ at 298 K is 0.26‰ larger than that of $Cu(H_2O)_6^{2+}$.
312

313 *3.3.2. Hydrated Cu(II) chlorides*

314 The structure of the hydrated Cu(II) chloride $CuCl_m(H_2O)_n^{2-m}$ is shown in
315 Tables 6 and S1 together with literature values. For the Cu(II) *monochloride*, $CuCl^+$,
316 both fivefold (D'Angelo et al., 1997) and sixfold (Rode and Islam, 1992; Texler et al.,
317 1998) coordination have been reported. The bond distances obtained for the
318 fivefold-coordinated $CuCl(H_2O)_4^+$ reproduce the experimental results of D'Angelo et al.
319 (1997). Though the geometry of sixfold-coordinated $CuCl(H_2O)_5^+$ was optimized within
320 the SCF convergence criterion, this species still showed a few imaginary (negative)
321 frequencies. Tighter convergence criteria may be needed.

322 The Jahn-Teller effect should be detectable in the sixfold-coordinated Cu(II)
323 *dichloride*, $CuCl_2(H_2O)_4$. For a geometry with an axial Cl-Cu-Cl bond, we found two
324 long and two short Cu-O bonds in the equatorial plane (Fig. 2). Our calculation agreed
325 with the bond distances determined experimentally (Neilson, 1982; Tajiri and Wakita,
326 1986). A fivefold coordinated structure was inferred from the experiments of Ansell et
327 al. (1995), and, indeed, we found evidence for a stable fivefold-coordinated
328 $CuCl_2(H_2O)_3$ structure with a distorted square pyramid (Fig. 2).

329 The X-ray diffraction study of Bell et al. (1973) reports the existence of
330 sixfold-coordinated Cu(II) *trichloride*, $CuCl_3(H_2O)_3^-$, which is an average structure of
331 polymerized Cu(II) chlorides in a concentrated $CuCl_2$ solution. The complex has three
332 Cu-Cl and three Cu-O bonds, a very low symmetry, and is unstable. The isolated $CuCl_3^-$
333 anion in solution may have a different structure. There are no reports in the literature of
334 the fivefold-coordinated $CuCl_3(H_2O)_2^-$. Convergence could not be achieved for the
335 square pyramidal nor the trigonal bipyramidal geometry. A smaller coordination
336 number was found for hydrated $CuCl_3^-$ (Collings et al., 2000). Under highly

337 concentrated HCl and $CuCl_2$ conditions, a higher order chlorinated $CuCl_4^{2-}$ exists. It is
338 disputed whether the structure is distorted octahedral $CuCl_4(H_2O)_2^{2-}$ or tetrahedral
339 $CuCl_4^{2-}$ (see references in Table 6). Systematic analysis by the extended X-ray
340 absorption fine structure (EXAFS) technique and Raman spectrometry suggested that a
341 possible structure is the tetrahedral $CuCl_4^{2-}$ (Tanimizu et al., 2007). This supports the
342 existence of fourfold-coordinated $CuCl_3H_2O^-$. The calculation of $CuCl_3H_2O^-$
343 successfully converged.

344 The ln β values of the hydrated chlorides are shown in Fig. 3 and Table 5. As
345 for the hydrated Cu^{2+} case, ln β (298 K) of the fivefold-coordinated $CuCl_2(H_2O)_3$ was
346 found to be 0.26‰ larger than that of the sixfold-coordinated $CuCl_2(H_2O)_4$. A
347 difference of this magnitude is assigned to a stereochemical effect. For the fivefold
348 coordination, the ln β value at 298 K for $Cu(H_2O)_5^{2+}$ is 0.56‰ larger than that of
349 $CuCl_2(H_2O)_3$ (Table 5). Likewise, for the sixfold coordination, the ln β value at 298 K
350 for $Cu(H_2O)_6^{2+}$ is also 0.56‰ larger than that of $CuCl_2(H_2O)_4$ (Table 5). This suggests
351 that, with the same coordination number, exchanging H_2O by Cl^- enhances $^{65}Cu/^{63}Cu$
352 fractionation by approximately the same amount.

353

354 As shown in Fig. 3, ln β decreases when the fraction of H_2O exchanged with
355 Cl^- increases. The variation of $\Delta^{65}Cu$ estimated from the ln β values (298 K) with the
356 molarity of HCl is shown in Fig. 1b. A similar observation was previously made for Ni
357 and Zn isotope fractionation (Fujii et al., 2010, 2011a).

358 The isotopic mass balance is preserved in the extraction system as,

$$\frac{\Sigma[^{65}Cu]}{\Sigma[^{63}Cu]} = \frac{[^{65}Cu^{2+}] + [^{65}CuCl^+] + [^{65}CuCl_2] + [^{65}CuCl_3^-] + [^{65}CuLCl_2]}{[^{63}Cu^{2+}] + [^{63}CuCl^+] + [^{63}CuCl_2] + [^{63}CuCl_3^-] + [^{63}CuLCl_2]} \quad (13)$$

359

360 The mole fractions of related Cu(II) species are evaluated from the values of K_{CuCl^+},

361 K_{CuCl_2}, $K_{CuCl_3^-}$ (Brugger, 2001), and *D* (Eq. 11), all obtained experimentally. Each mole

362 fraction is the sum of fractions of ^{63}Cu and ^{65}Cu isotopologues. The isotopic fractions

363 within the species were estimated from ln β. Since there is no structural information of

364 the Cu-DC18C6 complex in organic solution, β_{CuLCl_2} was set as a free parameter. The

365 results of the calculation are shown in Fig. 1b. The value of ln β_{CuLCl_2} converged to

366 3.35‰. The bold and dotted curves shown in Fig. 1b are the values of Δ^{65}Cu calculated

367 for ln β_{CuLCl_2} = 3.35 ± 0.05‰. The results agree well with the experimental results. An

368 important aspect of the estimation is that the calculation correctly predicts the sigmoidal

369 dependence of ln β on the fraction of H_2O exchanged by Cl^- with increasing HCl

370 molarity.

371

372 **3.4. Application to hydrous geochemistry**

373 In the absence of organic ligands which are known to dominate Cu speciation

374 in seawater (Moffet, 1995; Moffet and Brand, 1996; Hirose, 2006) the free Cu^{2+} ion is

375 dominant in freshwater, while the carbonate complexes $CuCO_3$ and $Cu(CO_3)_2^{2-}$ are

376 dominant in seawater (Albarède, 2004). Copper concentration in seawater increase

377 down the water column, which indicates both the uptake of Cu by plankton and

378 scavenging of Cu by settling particles (Boyle et al., 1977; Bruland, 1980). Dissolved Cu

379 in seawater is isotopically heavy (δ^{65}Cu = +0.9 to +1.5‰) relative to rocks and

380 sediments (0.0 to +0.3‰) and the riverine input (+0.69‰) (Bermin et al., 2006; Vance

381 et al., 2008). It was suggested that this result is attributable to the partitioning of Cu

382 isotopes between a heavy dissolved phase, where Cu is bound to organic ligands, and a
383 light particulate phase, dominated by Fe-Mn oxides (Vance et al., 2008). δ^{65}Cu in
384 Fe-Mn nodules (Albarède, 2004) and encrustations (Little et al., 2010) from the three
385 major ocean basins varies between +0.04 and +0.6‰, which is significantly lighter than
386 the δ^{65}Cu value in seawater (+0.9 to +1.5‰, Vance et al., 2008).

387 Surface seawater also contains various inorganic complexes and carbonates.
388 Speciation of Cu in seawater is very sensitive to the hydrolysis constants. Zirino and
389 Yamamoto (1972) used the cumulative formation constant of $Cu(OH)_2$, log β_2 = 14.3,
390 which, as shown in Fig. S1a (see the electronic supplement), makes Cu speciation in
391 seawater dominated by $Cu(OH)_2$. Mole fractions have been calculated from the set of
392 stability constants recommended by Powell et al. (2007) with the second hydrolysis
393 constant log $*\beta_2 = -16.65$, and the results are shown in Fig. 4a as a function of pH. At a
394 typical seawater pH of 8.22 (Macleod et al., 1994), $CuCO_3$ is the dominant species,
395 while the hydrated Cu^{2+} ion, chloride, sulfate, and hydroxide are subordinate. At pH ≥
396 8.22, $Cu(CO_3)_2^{2-}$ becomes an abundant species. These calculations are only relevant to
397 seawater with no organic ligands.

398 Figure 4b shows the isotope fractionation of Cu(II) among its various species
399 as estimated from their mole fractions and ln β (Tables 5 and 7) at 298 K under
400 conditions typical of seawater. The optimized geometries of the relevant species are
401 shown in Fig. 2 and Table S1 and the temperature dependence of ln β (Table 7) in Fig. 5.
402 The geometry of Cu hydroxides, $CuOH^+$ and $Cu(OH)_2$, were calculated by dissociating
403 H^+ ions from the *fivefold*-coordinated $Cu(H_2O)_5^{2+}$. The positions of OH^- ligands were
404 determined by reference to $CuCl^+$ and $CuCl_2$ (Fig. 2). The structure calculated for both

405 $CuOH(H_2O)_4^+$ and $Cu(OH)_2(H_2O)_3$ converged to a distorted square pyramid. With a
406 H_2O molecule at the vertex of the square pyramid, the bond distance is shorter for
407 $Cu\text{-}OH^-$ (1.8-1.9 Å) than for $Cu\text{-}OH_2$ (2.3-2.4 Å) (see Table S1). This suggests that the
408 stronger Cu-O bonds on the square plane loosen the hydration bond from the vertex.
409 This conclusion is consistent with the known structure of amorphous $Cu(OH)_2$ or
410 $Cu(OH)_2$ colloidal solution, which both show a layer structure of polymerized square
411 planes (Elizarova et al., 1999; Kriventsov et al., 1999).

412 *Fourfold* complexation occurs in both amorphous and crystalline $Cu(OH)_2$. A
413 stable fourfold complexation was also obtained for the Cu(II) carbonates, $CuCO_3(H_2O)_2$
414 and $Cu(CO_3)_2^{2-}$ (Fig. 2 and Table S1). CO_3^{2-} was treated as a bidentate ligand. The
415 structure converged to a distorted square plane. We tested positioning a water molecule
416 above the plane in the initial structure, but it moved out of the inner coordination shell
417 during the calculation. The structural optimization of $CuCO_3OH^-$ was more problematic.
418 Since CO_3^{2-} and OH^- occupy three coordination positions, one water molecule should
419 also bind to Cu(II) at the fourth coordination position, thereby giving the
420 $CuCO_3(OH)H_2O^-$ compound. It was actually found that no water molecule is stable in
421 the inner coordination shell. From the stoichiometry, the stable model molecule may
422 instead be $CuHCO_3(OH)_2^-$. This stable structure, in which HCO_3^- acts as a
423 quasi-bidentate ligand is shown in Fig. 2 and Table S1. The ln β values obtained are
424 shown in Fig. 5 and Table 7. The Cu hydroxides and carbonates have ln β values of
425 4.3-5.2‰ (298 K), in which compounds with higher complexation with OH^- and CO_3^{2-}
426 resulted in ln $\beta \geq 5$‰ (298 K).

427 The structure of hydrated Cu(II) in sulfate solutions was previously
428 investigated by Ohtaki et al. (1976) and Musinu et al. (1983). In $CuSO_4$ solutions, Cu^{2+}

429 is surrounded by disordered ligands (Musinu et al., 1983), which suggests a direct
430 interaction of Cu^{2+} with SO_4^{2-}. We used the structural model of Fe(III) sulfate proposed
431 by Magini (1979) as a reference for $CuSO_4(H_2O)_4$ (Fig. 2 and Table S1), in which SO_4^{2-}
432 is treated as a monodentate ligand, and obtained bond distances of 1.9-2.1 Å for
433 Cu-OH_2 and 2.37 Å for Cu-OSO_3^{2-}. These values agree with the Cu-O bond distances
434 determined by X-ray diffraction (Musinu et al., 1983). The electron donor SO_4^{2-}
435 strongly attracts H^+ and the resulting structure is equivalent to $CuH_2SO_4(OH)_2$ (Fig. 2).
436 The magnitude of ln β for $CuSO_4$ is 5.14‰ at 298 K (Table 7) and matches that of
437 $Cu(CO_3)_2^{2-}$ (Fig. 5).

438 As shown in Figs. 4a and 4b, at pH ≥ 8.22, the dominant Cu(II) species are
439 carbonates. We found that Cu in $Cu(CO_3)_2^{2-}$ (and $CuSO_4$) is isotopically 0.6‰ heavier
440 than Cu^{2+} ion. At pH = 8.22, the δ^{65}Cu value of $CuCO_3$ is slightly negative –0.17‰,
441 whereas those of $Cu(CO_3)_2^{2-}$ and $CuCO_3OH^-$ are substantially heavier, 0.75‰ and
442 0.58‰, respectively. At high pH, the relevant fractionation factors are
443 $\Delta^{65}Cu[Cu(CO_3)_2^{2-}\text{-}CuCO_3] = 0.92‰$ and $\Delta^{65}Cu[CuCO_3OH^-\text{-}CuCO_3] = 0.75‰$. Copper
444 in carbonates, whether in $CuCO_3$ or in solid solutions with carbonates of other elements
445 should therefore be isotopically light with respect to dissolved Cu.

446 At pH = 8.22, $Cu(OH)_2$ is +0.48‰ heavier than bulk seawater Cu (Fig. 4b). A
447 caveat is the somewhat different fractionation obtained when the cumulative formation
448 constant of $Cu(OH)_2$, log β_2 =14.3 of Zirino and Yamamoto (1972) is used. The major
449 species are $Cu(OH)_2$ and $CuCO_3$, while mole fractions of other species are insignificant
450 (Fig. S1a, Zirino and Yamamoto, 1972). The δ^{65}Cu shift of $Cu(OH)_2$ and $CuCO_3$ at pH
451 = 8.22 with respect to dissolved Cu are +0.02‰ and –0.62‰, respectively (Fig. S1b).

Isotope fractionation may therefore not be seen in Cu(II) hydroxide, but Cu in $CuCO_3$ should nevertheless remain isotopically light with respect to the seawater value.

As sulfides have small ln β values (Fujii et al., 2011b; Pons et al., 2011), sulfate-sulfide and carbonate-sulfide exchange are possibly determinant reactions for Cu isotope fractionation in seawater. $CuHS(H_2O)_4^+$ and $Cu(HS)_2(H_2O)_3$ were calculated with the geometries shown in Table S1. The structures that successfully converged were similar to those of the hydroxides shown in Fig. 2. The ln β values are shown in Fig 5 and Table 7. It is clear that the ln β values of Cu(II) sulfides are smaller than those of all the species shown in Fig. 3. In particular, the ln β values of Cu sulfides are 1.9-2.0‰ smaller than those of Cu sulfate and carbonates. Diagenetic Cu(II)-bearing sulfides are expected to be isotopically lighter than dissolved Cu, while Cu in the water table of sulfide-rich terranes should be heavy (Mathur et al., 2005, 2012).

Isotope fractionation also occurs under reducing conditions through Cu(I)-Cu(II) redox reactions. The ln β values calculated for Cu(I) chlorides and hydrogensulfides are ≤ 2.6‰ at 298 K (Seo et al., 2007), which suggests that Cu(I) complexes preferentially enrich ^{63}Cu and their precipitation results in the enrichment of ^{65}Cu in the fluid.

Cu in sulfides should be isotopically light with respect to dissolved aqueous Cu, and the main form of Cu removal from aquatic systems is Cu sulfide. The heavy isotopic composition of Cu in surface seawater (Vance et al., 2008) and groundwater (Mathur et al., 2012) therefore likely reflects that Cu carbonate complexes are held back in solution, while Cu is precipitated in sulfides. Complexation of Cu(II) with organic matter in surface seawater (Moffett, 1995) should also cause Cu isotope fractionation.

475 Evidence for the large-scale deposition of sediments with isotopically light Cu required
476 by mass balance is, however, still missing.
477
478 **3.5. Application to biological activity**
479 A variety of biological processes may induce Cu isotope fractionation.
480 Pokrosvky et al. (2008) demonstrated that Cu in bacteria is isotopically light relative to
481 the ambient solution. Pokrovsky et al. (2012) further identified S-coordinated Cu(I)
482 complexes at the surface and inside bacterial cells that may preferentially concentrate
483 ^{63}Cu over ^{65}Cu. It is therefore appealing to assign isotope fractionation in biological
484 material to competing Cu(II) and Cu(I) complexation. Mammal physiology is also a
485 cause of Cu isotope fractionation. Albarede et al. (2011a) found a ~1‰ fractionation
486 between human erythrocytes and serum. High δ^{65}Cu values of 1.5‰ were found in the
487 kidney of both sheep (Balter and Zazzo, 2011) and mice (Albarède et al., 2011b) with
488 respect to the rest of the body.
489 Oxalic acid is an ubiquitous toxic organic acid in body fluids. Oxalate is
490 adsorbed in the intestinal track, but the question of the origin of high oxalate contents in
491 urine and plasma found in patients prone to kidney damage is still contentious. This is a
492 genuine medical concern as ascorbate (vitamin C) supplementation has been argued to
493 increase the urinary oxalate levels, and therefore ascorbate may be a risk factor for
494 individuals predisposed to kidney stones (Chai et al., 2005; González et al., 2005;
495 Massey et al., 2005). Ascorbate is efficiently converted to oxalate when the coexisting
496 copper concentration is high (Hayakawa et al., 1973).
497 Hayakawa et al. (1973) suggest that Cu(II) is readily reduced by ascorbic acid
498 (H_2A) to Cu(I),

$$H_2A + 2Cu(II) \rightarrow A + 2Cu(I) + 2H^+ \quad (14)$$

499

500 The ascorbate anion A^{2-} here is oxidized to A, dehydroascorbic acid $C_6H_6O_6$. In the
501 catalytic reaction by a multicopper oxidase, ascorbate oxidase, the oxidation of
502 ascorbate to dehydroascorbate occurs via the disproportionation of the
503 semidehydroascorbate radical (Solomon et al., 1996). The enzymatic reactions may be
504 identical to the catalytic reaction 14.

505 The monohydroascorbate anion HA^- forms a complex with Cu^{2+}, $CuHA^+$.

$$Cu^{2+} + HA^- \rightleftarrows CuHA^+, \quad K_{CuHA^+} \quad (15)$$

506

507 Degradation of ascorbate via dehydroascorbate forms oxalate. A pathway of ascorbate
508 degradation has been proposed by Green and Fry (2005).

509 The oxalic acid also forms a complex with Cu^{2+}, CuC_2O_4.

$$Cu^{2+} + C_2O_4^{2-} \rightleftarrows CuC_2O_4, \quad K_{CuC_2O_4} \quad (16)$$

510

511 The value of the standard redox potential Eh with respect to the standard hydrogen
512 electrode (SHE), E_0, for the Cu redox reaction,

$$Cu^+ \rightleftarrows Cu^{2+} + e^- \quad (17)$$

513

514 is $E_0 = 0.153 + 0.591 \log ([Cu^{2+}]/[Cu^+])$ (Pourbaix, 1974). We used the following acid
515 dissociation constants and equilibrium constants $pK_a = 4.03$ (ascorbic acid), $pK_{a1} =$
516 1.252, $pK_{a2} = 4.266$ (oxalic acid) (Smith and Martell, 1989), $\log K_{CuHA^+} = 2.32$

517 (Jameson et al., 1976), and log $K_{CuC_2O_4}$ = 4.5 (Foreci et al., 1995). Figure 6a shows the
518 mole fractions of Cu^+, Cu^{2+}, $CuHA^+$, and CuC_2O_4 as functions of Eh. The total
519 concentrations of Cu and ascorbic acid are ~10^{-6} M (Lech and Sadlik, 2007) and ~10^{-4}
520 M (Margolls and Davis, 1988), respectively. The pH and Eh in the body are known to
521 be ~7.4 and 0.27 V (van Rossum and Schamhart, 1991). These values were used to
522 estimate the mole fractions of Cu species using the assumption that 10% of ascorbic
523 acid is converted to oxalic acid. We further assumed that no other degradation products
524 were present. Figure 6b shows the speciation as a function of the reaction progress. As
525 expected, oxidation of Cu(I) to Cu(II) proceeds with increasing Eh, which in turn
526 enhances Cu-ascorbate and Cu-oxalate formation. The degradation of ascorbate
527 increases oxalic acid concentration and therefore promotes the production of
528 Cu-oxalate.

529 Figure 6c and 6d show the range of isotope fractionation among Cu species as
530 estimated from their mole fractions and ln β at 298 K (Tables 5 and 8). The optimized
531 geometries of related species are shown in Table S1. Hydrated Cu^+ was treated as free
532 Cu(I). Cu(I) complexes possess simple linear structures (Fulton et al., 2000a,b). Our ln
533 β value of 2.87‰ at 289K for $Cu(H_2O)_2^+$ (Table 8) is consistent with the value of
534 2.89‰ estimated by *ab initio* methods for $CuClH_2O$ (Seo et al., 2007). $Cu(H_2O)_5^{2+}$ was
535 treated as free Cu(II), and its ln β is given in Table 5. For the geometry of Cu(II)
536 ascorbate $CuHA^+$, we used the copper monomer (Ünaleroğlu et al., 2001). The structure
537 calculated for Cu(II) in fivefold coordination with L-ascorbate and H_2O is shown in Fig.
538 2 and Table S1. The value of ln β calculated at 298 K is 3.32‰. The ln β value of
539 D-ascorbate at 298 K (also 3.38‰) is indistinguishable from that of L-ascorbate. The

geometry of Cu(II) oxalate was quite similar to the structure of the hydrated Cu carbonate. It successfully converged to a distorted plane configuration (Fig. 2 and Table S1) and led to large ln β values (Fig.7 and Table 8).

Figures 6c and 6d show the δ^{65}Cu values of the different species relative to the bulk solution as a function of Eh and extent of oxalate formation. Figure 6c shows that, with respect to free Cu(II), free Cu(I) is enriched in the light isotope. When Cu(I) and Cu(II) coexist, the δ^{65}Cu of the total free Cu ions is only slightly lighter than the sum of all the Cu species. The δ^{65}Cu of the Cu ascorbate varies from –1.0 to +0.5‰ when Eh increases from –1 V to +1 V, but its mole fraction remains very small. The prominent feature of Fig. 6c is the heavy isotope enrichment (+0.6 to +2.5‰) of the Cu oxalate relative to total Cu. Figure 6d was drawn for Eh = 0.27 V, which is a typical Eh value of human blood. It is expected that degradation of ascorbate and excretion of oxalate should leave isotopically heavy Cu in the kidney. With respect to food, which has a δ^{65}Cu value of about 0‰ (Balter and Zazzo, 2011), when even trace amounts of oxalate form, it should leave behind copper with a δ^{65}Cu of ~1.4‰. This value is very close to the δ^{65}Cu (of 1.5‰) found in sheep (Balter and Zazzo, 2011) and mice (Albarède et al., 2011b) kidneys. The positive δ^{65}Cu found in kidneys may result from isotopically heavy Cu left in the kidney by the degradation of ascorbic acid. Copper isotopes therefore represent a potential marker of the troubles associated with hyperoxalury and kidney stones.

4. CONCLUSIONS

562 We first demonstrated that Cu isotope fractionation at equilibrium is observed in
563 laboratory-scale experiments. The effect on the $^{65}Cu/^{63}Cu$ ratio of Cu(II) partitioning
564 between HCl and DC18C6 depends on acid molarity. The effect is mainly governed by
565 the mass-dependent fractionations as a result of intramolecular vibrations. The nuclear
566 field shift effect accounts for less than 3% of the mass-dependent fractionation. We then
567 computed the coefficients of isotope fractionation of Cu for several species (hydrated
568 Cu ion, hydroxide, chloride, sulfide, sulfate, carbonate, oxalate, and ascorbate). It was
569 found that Cu in dissolved carbonates and sulfates is isotopically heavier than free Cu
570 and Cu in sulfides. The theoretical estimation of $\delta^{65}Cu$ in ligand exchange between
571 inorganic ligands including carbonate anions may be useful to understand the heavy Cu
572 isotopic compositions found in both seawater and groundwater in the absence of strong
573 organic ligands. Further theoretical estimation of $\delta^{65}Cu$ in hydrated Cu(I) and Cu(II)
574 ions, Cu(II) ascorbates, and Cu(II) oxalate suggests that Cu isotope fractionation during
575 the breakdown of ascorbate into oxalate results in the isotopically heavy Cu found in
576 mammal kidneys.
577

578 **ACKNOWLEDGMENT**

579 The authors thank the anonymous reviewers and Associate Editor Mark
580 Rehkämper for their useful suggestions and constructive comments on the manuscript.
581 The authors wish to thank the generous help of Janne Blichert-Toft in editing the
582 English of this paper. FM acknowledged the support of NASA EXO (NNX12AD88G)
583 and of the Washington University I-CARES program.
584

585 **REFERENCES**

586 Abe M., Suzuki T., Fujii Y., Hada M. and Hirao K. (2008) An *ab* initio molecular
587 orbital study of the nuclear volume effects in uranium isotope fractionations. *J. Chem.*
588 *Phys*. **129**, 164309.

589 Abe M., Suzuki T., Fujii Y., Hada M., Hirao K. (2010) Ligand effect on uranium
590 isotope fractionations caused by nuclear volume effects: An ab initio relativistic
591 molecular orbital study. *J. Chem. Phys*. **133**, 044309.

592 Åkesson R., Pettersson L. G. M., Sandström M. and Wahlgren U. (1992) Theoretical
593 calculations of the Jahn-Teller effect in the hexahydrated copper(II), chromium(II),
594 and manganese(III) ions, $[Cu(H_2O)_6]^{2+}$, $[Cr(H_2O)_6]^{2+}$, and $[Mn(H_2O)_6]^{3+}$, and
595 comparisons with the hexahydrated copper(I), chromium(III), and manganese(II)
596 clusters. *J. Phys. Chem*. **96**, 150-156.

597 Albarède F. (2004) The stable isotope geochemistry of copper and zinc. *Rev. Mineral.*
598 *Geohem*. **55**, 409-427.

599 Albarède F., Telouk P., Lamboux A., Jaouen K. and Balter V. (2011a) Isotopic evidence
600 of unaccounted for Fe and Cu erythropoietic pathways. *Metallomics* **3**, 926-933.

601 Albarède F., Balter V., Jaouen K. and Lamboux A. (2011b) Applications of the stable
602 isotopes of metals to physiology. *The 38th Meeting of the Federation of Analytical*
603 *Chemistry and Spectroscopy Societies (FACSS)*, Reno (abstract).

604 Amira S., Spångberg D. and Hermansson K. (2005) Distorted five-fold coordination of
605 Cu^{2+}(aq) from a Car-Parrinello molecular dynamics simulation. *Phys. Chem. Chem.*
606 *Phys*. 7, 2874-2880.

607 Angeli I. (2004) A consistent set of nuclear rms charge radii: properties of the radius
608 surface R(N,Z). *At. Data Nucl. Data Tables* **87**, 185-206.

609 Ansell S., Tromp R. H. and Neilson G. W. (1995) The solute and aquaion structure in a
610 concentrated aqueous solution of copper(II) chloride. *J. Phys.: Condens. Matter* **7**,
611 1513-1524.
612 Archer C. and Vance D. (2002) Mass discrimination correction in multiple collector
613 plasma source mass-spectrometry: an example using Cu and Zn isotopes. *J. Anal. At.*
614 *Spectrom*. **64**, 356-365.
615 Balistrieri L. S., Borrok D. M., Wanty R. B. and Ridley W. I. (2008) Fractionation of
616 Cu and Zn isotopes during adsorption onto amorhous Fe(III) oxyhydroxide:
617 Experimental mixing of acid rock drainage and ambient river water. *Geochim.*
618 *Cosmochim. Acta* **72**, 311-328.
619 Balter V. and Zazzo A. (2011) An animal model (sheep) for Fe, Cu, and Zn isotopes
620 cycling in the body. *Mineralogical Magazine* **75**, 476-476.
621 Beagley B., Eriksson A., Lindgren J., Persson I, Pettersson L. G. M., Sandström M.,
622 Wahlgren U. and White E. W. (1989) A computational and experimental study on
623 the Jahn-Teller effect in the hydrated copper (II) ion. Comparisons with hydrated
624 nickel (II) ions in aqueous solution and solid Tutton's salts. *J. Phys.: Condens. Matter*
625 **1**, 2395-2408.
626 Becke A. D. (1993) Density-functional thermochemistry. 3. The role of exact exchange.
627 *J. Chem. Phys*. **98**, 5648-5652.
628 Benfatto M., D'Angelo P., Della Longa S. and Pavel N. V. (2002) Evidence of distorted
629 fivefold coordination of the Cu^{2+} aqua ion from an x-ray-absorption spectroscopy
630 quantitative analysis. *Phys. Rev. B* **65**, 174205.
631 Bell J. R., Tyvoll J. L. and Wertz D. L. (1973) Solute structuring in aqueous copper(II)
632 chloride solutions. *J. Am. Chem. Soc*. **95**, 1456-1459.

633 Ben Othman D., Luck J. M., Bodinier J. L., Arndt N. T. and Albarède F. (2006) Cu-Zn
634 isotopic variations in the Earth's mantle. *Geochim. Cosmochim. Acta Suppl*. **70**,
635 46-46.
636 Bermin J., Vance D., Archer C. and Statham P.J. (2006) The determination of the
637 isotopic composition of Cu and Zn in seawater. *Chem. Geol*. **226**, 280-297.
638 Bersuker I. B. (2006) *The Jahn-Teller effect*; Cambridge Univ. Press, New York.
639 Bigalke M., Weyer S. and Wilcke W. (2010) Stable copper isotopes: a novel tool to
640 trace copper behavior in hydromorphic soils. *Soil Sci. Soc. Am. J*. **74**, 60-73.
641 Bigalke M., Weyer S. and Wilcke W. (2011) Stable Cu isotope fractionation in soils
642 during oxic weathering and podzolization. *Geochim. Cosmochim. Acta* **75**,
643 3119-3134.
644 Bigeleisen J. and Mayer M. G. (1947) Calculation of equilibrium constants for isotopic
645 exchange reactions. *J. Chem. Phys*. **15**, 261-267.
646 Bigeleisen J. (1996) Nuclear size and shape effects in chemical reactions. isotope
647 chemistry of the heavy elements. *J. Am. Chem. Soc*. **118**, 3676-3680.
648 Bishop M. C., Moynier F., Weinstein C., Fraboulet J. G., Wang K. and Foriel J. (2012)
649 Cu isotopic composition of iron meteorites. *Meteor. Planet. Sci*. **47**, 268-276.
650 Black J. R., Kavner A. and Schauble E. A. (2011) Calculation of equilibrium stable
651 isotope partition function ratios for aqueous zinc complexes and metallic zinc.
652 *Geochim. Cosmochim. Acta* **75**, 769-783.
653 Boyle E. A., Sclater F. R. and Edmond J.M. (1977) The distribution of dissolved copper
654 in the Pacific. *Earth Planet. Sci. Lett*., **37**, 38-54.
655 Breza M., Biskupic S. and Kozisek J. (1997) On the structure of hexaaquacopper(II)
656 complex. *J. Mol. Struct. (Teochem)* **397**, 121-128.

657 Brugger J., M$_C$Phail D. C., Black J and Spiccia L. (2001) Complexation of metal ions in
658 brines: application of electronic spectroscopy in the study of the Cu(II)-LiCl-H2O
659 system between 25 and 90°C. *Geochim. Cosmochim. Acta* **6**5, 2691.
660 Bruland K.W. (1980) Oceanographic distributions of cadmium, zinc, nickel, and copper
661 in the North Pacific. *Earth Planet. Sci. Lett*. **47**, 176-198.
662 Bryantsev V. S., Diallo M. S., van Duin A. C. T. and Goddard III W. A. (2008)
663 Hydration of copper(II): new insights from density functional theory and the COSMO
664 solvation model. *J. Phys. Chem. A* **112**, 9104-9112.
665 Chaboy J., Muñoz-Páez A., Merkling P. J. and Sánchez Marcos E. (2006) The hydration
666 of Cu^{2+}: Can the Jahn-Teller effect be detected in liquid solution? *J. Chem. Phys*. **124**,
667 064509.
668 Chai W., Liebman M., Kynast-Gales S. and Massey L. (2004) Oxalate absorption and
669 endogenous oxalate synthesis from ascorbate in calcium oxalate stone frmers and
670 non-stone formers. *Am. J. Kedney Diseases* **44**, 1060-1069.
671 Collings M. D., Sherman D. M. and Ragnarsdottir K. V. (2000) Complexation of Cu^{2+}
672 in oxidized NaCl brines from 25°C to 175°C: results from in situ EXAFS
673 spectroscopy. *Chem. Geol*. **167**, 65-73.
674 Contreras F., Fontal B. and Bianchi G. (1993) Copper(II) thiocyanide complexes
675 extractable with [dibenzo-18-crown-6-K]$^+$ in chloroform. *Transition Met. Chem*. **18**,
676 104-106.
677 Cowan J.A. (1997) *Inorganic Biochemistry*, Wiley-VCH, New York.
678 de Almeida K. J., Murugan N. A., Rinkevicius Z., Hugosson H. W., Vahtras O., Ågrena
679 H. and Cesar A. (2009) *Phys. Chem. Chem. Phys*. **11**, 508-519.

680 de Bruin T. J. M., Marcelis A. T. M., Zuilhof H. and Sudhölter E. J. R. (1999)
681 Geometry and electronic structure of bis-(glycinato)-$Cu^{II}\cdot 2H_2O$ complexes as studied
682 by density functional B3LYP computations. *Phys. Chem. Chem. Phys*. **1**, 4157-4163.
683 Dennington R., Keith T. and Millam J. (2009) *GaussView, Version 5.0.8*. Semichem
684 Inc., Shawnee Mission KS.
685 Eigen M. (1963) Fast elementary steps in chemical reaction mechanisms. *Pure Appl.*
686 *Chem*. **6**, 97-116.
687 Elizarova G. L., Kochubey D. I., Kriventsov V. V., Odegova G. V., Matvienko H. L. G.,
688 Kolomiychuk V. N. and Parmon V. N. (1999) Study of the interaction products of
689 some N- and O-containing compounds with highly dispersed copper(II) hydroxide. *J.*
690 *Colloid Interface Sci*. **213**, 126-132.
691 Epov V. N., Malinovskiy D., Vanhaecke F., Begue D. and Donard O. F. X. (2011)
692 Modern mass spectrometry for studying mass-independent fractionation of heavy
693 stable isotopes in environmental and biological sciences. *J. Anal. At. Spectrom*. **26**,
694 1142-1156.
695 Epov V. N (2011) Magnetic isotope effect and theory of atomic orbital hybridization to
696 predict a mechanism of chemical exchange reactions. *Phys. Chem. Chem. Phys*. **13**,
697 13222-13231.
698 Faegri K. (2001) Relativistic Gaussian basis sets for the elements K-Uuo. *Theo. Chem.*
699 *Acc.* **105**, 252-258.
700 Feroci G., Fini A., Fazlo G. and Zuman P. (1995) Interaction between dihydroxy bile
701 salts and divalent heavy metal ions studied by polarography. *Anal. Chem*. **67**,
702 4077-4085.

703 Freeman H. C. and Guss J. M. (2001) Plastocyanin. In *Handbook of Metalloproteins*
704 (eds. R. Huber, T. L. Poulos, and K. Wieghardt), Wiley, Chichester. pp. 1153-1169.
705 Frisch M. J., Trucks G. W., Schlegel H. B., Scuseria G. E., Robb M. A., Cheeseman J.
706 R., Scalmani G., Barone V., Mennucci B., Petersson G. A., Nakatsuji H., Caricato M.,
707 Li X., Hratchian H. P., Izmaylov A. F., Bloino J., Zheng G., Sonnenberg J. L., Hada
708 M., Ehara M., Toyota K., Fukuda R., Hasegawa J., Ishida M., Nakajima T., Honda Y.,
709 Kitao O., Nakai H., Vreven T., Montgomery Jr. J. A., Peralta J. E., Ogliaro F.,
710 Bearpark M., Heyd J. J., Brothers E., Kudin K. N., Staroverov V. N., Kobayashi R.,
711 Normand J., Raghavachari K., Rendell A., Burant J. C., Iyengar S. S., Tomasi J.,
712 Cossi M., Rega N., Millam N. J., Klene M., Knox J. E., Cross J. B., Bakken V.,
713 Adamo C., Jaramillo J., Gomperts R., Stratmann R. E., Yazyev O., Austin A. J.,
714 Cammi R., Pomelli C., Ochterski J. W., Martin R. L., Morokuma K., Zakrzewski V.
715 G., Voth G. A., Salvador P., Dannenberg J. J., Dapprich S., Daniels A. D., Farkas Ö.,
716 Foresman J. B., Ortiz J. V., Cioslowski J. and Fox D. J. (2009) *Gaussian 09, Revision*
717 *B.01*, Gaussian, Inc., Wallingford CT.
718 Fujii T., Moynier F., Telouk P. and Albarede F. (2006) Isotope fractionation of iron(III)
719 in chemical exchange reactions using solvent extraction with crown ether. *J. Phys.*
720 *Chem. A* **110**, 11108-11112.
721 Fujii T., Moynier F. and Albarède F. (2009) The nuclear field shift effect in chemical
722 exchange reactions. *Chem. Geol*. **267**, 139-156.
723 Fujii T., Moynier F., Telouk P. and Abe, M. (2010) Experimental and theoretical
724 investigation of isotope fractionation of zinc between aqua, chloro, and macrocyclic
725 complexes. *J. Phys. Chem. A* **114**, 2543-2552.

726 Fujii T. Moynier F., Dauphas N. and Abe M. (2011a) Theoretical and experimental
727 investigation of nickel isotopic fractionation in species relevant to modern and
728 ancient oceans. *Geochim. Cosmochim. Acta* **75**, 469-482.
729 Fujii T., Moynier F. Pons M. L. and Albarède F (2011b) The origin of Zn isotope
730 fractionation in sulfides. *Geochim. Cosmochim Acta* **75**, 7632-7643.
731 Fujii T., Moynier F., Agranier A., Ponzevera E. and Abe M. (2011c) Nuclear field shift
732 effect of lead in ligand exchange reaction using a crown ether. *Proc. Radiochim. Acta*.
733 **1**, 387-392.
734 Fujii T., Moynier F., Agranier A., Ponzevera E. and Abe M. (2011d) Isotope
735 fractionation of palladium in chemical exchange reaction. *Proc. Radiochim. Acta*. **1**,
736 339-344.
737 Fujii T. and Albarède F. (2012) Ab initio calculation of the Zn isotope effect in
738 phosphates, citrates, and malates and applications to plants and soil. *PLoS ONE* **7**,
739 e30726.
740 Fulton J. L., Hoffmann M. M. and Darab J. G. (2000a) An x-ray absorption fine
741 structure study of copper(I) chloride coordination structure in water up to 325°C.
742 *Chem. Phys. Lett*. **330**, 300-308.
743 Fulton J. L., Hoffmann M. M., Darab J. G., Palmer B. J. and Stern E. A. (2000b)
744 Copper(I) and copper(II) coordination structure under hydrothermal conditions at
745 325°C: an x-ray absorption fine structure and molecular dynamics study. *J. Phys.*
746 *Chem. A* **104**, 11651-11663.
747 Garcia J., Benfatto M. Notoli C. R., Bianconi A., Fontaine A. and Tolentino H. (1989)
748 The quantitative Jahn-Teller distortion of the Cu2+ site in aqueous solution by
749 XANES spectroscopy. *Chem. Phys*. **13**2, 295-307.

González M. J., Miranda-Massari J. R., Mora E. M., Guzmán A., Riordan N. H., Riordan H. D., Casciari J. J., Jackson J. A. and Román-Franco A. (2005) Orthomolecular oncology review: Ascorbic acid and cancer 25 years later. *Integr. Cancer Ther*. **4**, 32-44.

Green M. A. and Fry S. C. (2005) Vitamin C degradation in plant cells via enzymatic hydrolysis of 4-O-oxalyl-L-threonate. *Nature* **433**, 83-87.

Hayakawa K., Minami S. and Nakamura S. (1973) Kinetics of the oxidation of ascorbic acid by the copper(II) ion in an acetate buffer solution. *Bull. Chem. Soc. Jpn*. **46**, 2788.

Herzog G. F., Moynier F. and Albarède F. (2009) Isotopic and elemental abundances of copper and zinc in. lunar basalts, glasses, and soils, a terrestrial basalt, Pele's hairs, and Zagami. *Geochim. Cosmochim. Acta*. **73**, 5884-5904.

Hill P. S., Schauble E. A. and Young E. D. (2010) Effects of changing solution chemistry on Fe^{3+}/Fe^{2+} isotope fractionation in aqueous Fe-Cl solutions. *Geochim. Cosmochim. Acta* **74**, 6669-6689.

Hirose K. (2006) Chemical speciation of trace metals in seawater: a review. *Anal. Sci*. **22**, 1055-1063.

Jameson R. F. and Blackburn N. J. (1976) Role of copper dimers and the participation of copper(III) in the copper-catalysed autoxidation of ascorbic acid. Part II. Kinetics and mechanism in 0.100 mol dm^{-3} potassium nitrate. *J. Chem. Soc., Dalton* 534-541.

Jepson B.E. and Cairns G.A. (1979) Lithium isotope effects in chemical exchange with (2,2,1) cryptand, *MLM-2622*.

772 Jouvin D., Weiss D. J., Mason T. F. M., Hinsinger P. and Benedetti M. F. (2012) Stable
773 isotopes of Cu and reduction at the root surface isotopic fractionation processes.
774 *Environ. Sci. Technol*. **46**, 2652-2660.
775 King W. H. (1984) *Isotope Shifts in Atomic Spectra*; Plenum Press, New York.
776 Klein S., Domergue C., Lahaye Y., Brey G. P. and von Kaenel H.-M. (2009) The lead
777 and copper isotopic composition of copper ores from the Sierra Morena (Spain). *J.*
778 *Iberian Geol.* **35**, 59-68.
779 Koc K. and Ishikawa Y. (1994) Single-Fock-operator method for matrix Dirac-Fock
780 self-consistent-field calculations on open-shell atoms. *Phys. Rev. A* **49**, 794-798.
781 Kriventsov V. V., Kochubey D. I., Elizarova G. L., Matvienko H. L. G. and Parmon V.
782 N. (1999) The structure of amorphous bulk and silica-supported copper(II)
783 hydroxides. *J. Colloid Interface Sci*. **215**, 23-27.
784 Lec T. and Sadlik J. K. (2007) Contribution to the data on copper concentration in blood
785 and urine in patients with Wilson's disease and in normal subjects. *Biol. Trace Elem.*
786 *Res*. 118, 16-20.
787 Lee C. T., Yang W. T. and Parr R. G. (1988) Development of the colle-salvetti
788 correlation-energy formula into a functional of the electron-density. *Phys. Rev. B* **37**,
789 785-789.
790 Li W. Q., Jackson S. E., Pearson N. J., Alard O. and Chappell B. W. (2009) The Cu
791 isotopic signature of granites from the Lachlan Fold Belt, SE Australia. *Chem. Geol.*
792 **258**, 38-49.
793 Lippard S. J. and Berg J. M. (1994) *Principles of Bioinorganic Chemistry*, University
794 Science Books, Mill Valley.

795 Little S. H., Vance D., Sherman D. M. and Hein J.R. (2010) *Geochim. Cosmochim. Acta*
796 **74**, A608.
797 Liu X., Lu X., Meijer E. J. and Wang R. (2010) Hydration mechanisms of Cu^{2+}: tetra-,
798 penta- or hexa-coordinated? *Phys. Chem. Chem. Phys*. **12**, 10801-10804.
799 Macleod, G., Mcneown, C., Hall, A. J., Russel, M. J. (1994) Hydrothermal and oceanic
800 pH conditions of possible relevance to the origin of life. *Origin Life Evol. Biosphere*
801 **24**, 19-41.
802 Magini, M. (1979) Solute structuring in aqueous iron(III) sulphate solutions. Evidence
803 for the formation of iron(III)-sulphate complexes. *J. Chem. Phys*. **70**, 317-324.
804 Magini M. (1982) Coordination of copper(II). Evidence of the Jahn-Teller effect
805 inaqueous perchlorate solutions. *Inorg. Chem*. **21**, 1535-1538.
806 Maréchal C. N., Telouk P. and Albarède F. (1999) Precise analysis of copper and zinc
807 isotopic compositions by plasma-source mass spectrometry. *Chem. Geol.* **156**,
808 51-273.
809 Maréchal C. and Albarède F. (2002) Ion-exchange fractionation of copper and zinc
810 isotopes. *Geochim. Cosmochim. Acta* **66**, 1499-1509.
811 Marini G. W., Liedl K. R. and Rode B. M. (1999) Investigation of Cu^{2+} hydration and
812 the Jahn-Teller effect in solution by QM/MM Monte Carlo simulations. *J. Phys.*
813 *Chem. A* **103**, 11387-11393.
814 Margolls S. A and Davis T. P. (1988) Stabilizationof ascorbic acid in human plasma,
815 and its liquid-chromatographic measurement. *Clin. Chem*. **34**, 2217-2223.
816 Massey L. K., Liebman, M., Kynast-Gales S. A. (2005) Ascorbate increases human
817 oxaluria and kidney stone risk. *J. Nutrition* **135**, 1673-1677.

818 Mathur R., Ruiz J., Titley S., Liermann L., Buss H. and Brantley S. (2005) Cu isotopic
819 fractionation in the supergene environment with and without bacteria. *Geochim. Cosmochim. Acta* **69**, 5233-5246.
821 Mathur R. Jin L., Prush V., Paul J., Ebersole C., Fornadel A., Williams J. Z. and
822 Brantley S. (2012) Cu isotopes and concentrations during weathering of black shale
823 of the Marcellus Formation, Huntingdon County, Pennsylvania (USA). *Chem. Geol*.
824 **304-305**, 175-184.
825 Matin M. D. A., Nomura M., Fujii Y. and Chen J. (1998) Isotope effects of copper in
826 ligand-exchange system and electron-exchange system observed by ion-exchange
827 displacement chromatography. *Sep. Sci. Technol*. **33**, 1075-1087.
828 Moffett J. W. (1995) Temporal and spatial variability of copper complexation by strong
829 chelators in the Sargasso Sea. *Deep Sea Res I* **42**, 1273-1295.
830 Moffett J. W. and Brand L. E. (1996) The production of strong, extracellular Cu
831 chelators by marine cyanobacteria in response to Cu stress. *Limnol. Oceanogr*. **41**,
832 388-395.
833 Morel F. M. M. and Hering J. G. (1993) *Principles and Applications of Aquatic*
834 *Chemistry*, John Wiley, New York.
835 Moynier F., Koeberl C., Beck P., Jourdan F. and Telouk P. (2010) Isotopic fractionation
836 of Cu in tektites. *Geochim. Cosmochim. Acta* **74**, 799-807.
837 Musinu A., Paschina G., Piccaluga G. and Magini M. (1983) Coordination of copper(II)
838 in aqueous CuSO4 solution. *Inorg. Chem*. **22**, 1184-1187.
839 Nakamura E., Okubo K. and Namiki H. (1982) Butanol extraction of copper-zincon
840 complex with dibenzo-18-crown-6. *Bunseki Kagaku* **31**, 602-604.

841 Navarette J.U., Borrok D.M., Viveros M. and Ellzey J.T. (2011) Copper isotope
842 fractionation during surface adsorption and intracellular incorporation by bacteria.
843 *Geochim. Cosmochim. Acta* **75**, 784-799.
844 Neilson G. W. (1982) Cu^{2+} coordination in aqueous solution. *J. Phys. C: Solid State*
845 *Phys.* **15**, L233-L237.
846 Nishizawa K., Ishino S., Watanabe H. and Shinagawa M. (1984) Lithium isotope
847 separation by liquid-liquid extraction using benzo-15-crown-5. *J. Nucl. Sci. Technol*.
848 **21**, 694–701.
849 Nomura M., Higuchi N. and Fujii Y. (1996) Mass dependence of uranium isotope
850 effects in the U(IV)-U(VI) exchange reaction. *J. Am. Chem. Soc*. **118**, 9127-9130.
851 Nomura M. and Yamaguchi T. (1988) Concentration dependence of extended x-ray
852 absorption fine structure and x-ray absorption near-edge structure of copper(II)
853 perchlorate aqueous solution: comparison of solute structure in liquid and glassy
854 states. *J. Phys. Chem*. **92**, 6157-6160.
855 Ohtaki H and Maeda M. (1974) An x-ray diffraction study of the structure of hydrated
856 copper(II) ion in a copper(II) perchlorate solution. *Bull. Chem. Soc. Jpn*. **47**,
857 2197-2199.
858 Okan S. E. and Salmon P. S. (1995) The Jahn-Teller effect in solutions of flexible
859 molecules: a neutron diffraction study on the structure of a Cu^{2+} solution in ethylene
860 glycol. *Mol. Phys.* **85**, 981-998.
861 Pasquarello A., Petri I., Salmon P. S., Parisel O., Car R.,Toth E., Powell D. H., Fischer
862 H. E, Helm L. and Merbach A. E. (2001) First solvation shell of the Cu(II) aqua ion:
863 evidence for fivefold coordination. *Science* **291**, 856-859.

Persson I., Persson P., Sandström M. and Ullström A. -S. (2002) Structure of Jahn-Teller distorted solvated copper(II) ions in solution, and in solids with apparently regular octahedral coordination geometry. *J. Chem. Soc., Dalton Trans.* 1256-1265.

Pokrovsky O. S., Viers J., Emnova E. E., Kompantseva E. I. and Freydier R. (2008) Copper isotope fractionation during its interaction with soil and aquatic microorganisms and metal oxy(hyd)oxides: Possible structural control. *Geochim. Cosmochim. Acta* **72**, 1742-1757.

Pokrovsky O. S., Pokrovski G. S., Shirokova L. S., Gonzalez A. G., Emnova E. E. and Feurtet-Mazel A. (2012) Chemical and structural status of copper associated with oxygenic and anoxygenic phototrophs and heterotrophs: possible evolutionary consequences. *Geobiol*. **10**, 130-149.

Pons M. L., Quitté G., Fujii T., Rosing M. T., Reynard B., Moynier F., Douchet C. and and Albarède F. (2011) Early Archean serpentine mud volcanoes at Isua, Greenland, as a niche for early life. *Proc. Natl. Acad. Sci. USA* **108** 17639-17643.

Pourbaix, M. (1974) *Atlas of electrochemical equilibria in aqueous solutions.* NACE, Houston.

Rode B. M. and Islam S. M. (1992) Structure of aqueous copper chloride solutions: results from Monte Carlo simulations at various concentrations. *J. Chem. Soc., Faraday Trans.* **88**, 417-422.

Roos B. O., Lindh R., Malmqvist P. -Å., Veryazov V. and Widmark P. -O. (2005) New relativistic ANO basis sets for transition metal atoms. *J. Phys. Chem. A* **109**, 6575-6579.

887 Rustad J. R., Casey W. H., Yin Q. Z., Bylaska E. J., Felmy A. R., Bogatko S. A.,
888 Jackson V. E. and Dixon D. A. (2010) Isotopic fractionation of Mg^{2+}(aq), Ca^{2+}(aq),
889 and Fe^{2+}(aq) with carbonate minerals. *Geochim. Cosmochim. Acta* **74**, 6301-6323.
890 Salmon P. S. Neilson G. W. and Enderby J. E. (1988) The structure of Cu^{2+} aqueous
891 solutions. *J. Phys. C: Solid State Phys*. 21 1335-1349.
892 Schauble E. A. (2007) Role of nuclear volume in driving equilibrium stable isotope
893 fractionation of mercury, thallium, and other very heavy elements, *Geochim.*
894 *Cosmochim. Acta* **71**, 2170-2189.
895 Schwenk C. F. and Rode B. M. (2003a) New insights into the Jahn-Teller effect through
896 ab initio quantum-mechanical/molecular-mechanical molecular dynamics simulations
897 of Cu^{II} in water. *Chem. Phys. Chem*. **4**, 931-943.
898 Schwenk C. F. and Rode B. M. (2003b) Extended ab initio quantum
899 mechanical/molecular mechanical molecular dynamics simulations of hydrated Cu^{2+}.
900 *J. Chem. Phys*. **119**, 9523-9531.
901 Sherman D. M. (2001) Quantum chemistry and classical simulations of metal
902 complexes in aqueous solutions. *Rev. Mineral. Geochem*. **42**, 273-317.
903 Sham T. K., Hastings J. B. and Perlman M. L. (1981) Application of the EXAFS
904 method to Jhan-Teller ions: static and dynamic behavior of $Cu(H_2O)_6^{2+}$ and
905 $Cr(H_2O)_6^{2+}$ in aqueous solution. *Chem. Phys. Lett*. **83**, 391-396.
906 Shields W. R., Murphy T. J. and Garner E. L. (1964) Absolute isotopic abundance ratio
907 and the atomic weight of a reference sample of copper. *J. Res. NBS* 68A, 589-592.
908 Shields W. R., Goldich S. S., Garner E. L. and Murphy, T. J. (1965) Natural variations
909 in the abundance ratio and the atomic weight of copper. *J Geophys Res*, 7, 479-491.

910 Smith, R. M., Martell, A. E. (1989) *Critical stability constants*, vol. 6, 2nd Suppl.,
911 Plenum Press, New York.
912 Solomon E. I., Sundaram U. M and Machonkin T. E. (1996) Multicopper oxidases and
913 oxygenases. *Chem. Rev*. **96**, 2563-2605.
914 Tajiri Y. and Wakita H. (1986) An EXAFS investigation of the coordination structure of
915 copper(II) ions in aqueous $Cu(ClO_4)_2$ and mthanolic $CuCl_2$ solutions. Bull. Chem.
916 Soc. Jpn. 59, 2285-2291.
917 Tanimizu M., Takahashi Y. and Nomura M. (2007) Spectroscopic study on the anion
918 exchange behavior of Cu chloro-complexes in HCl solutions and its implication to Cu
919 isotopic fractionation. *Geochem. J*. **41**, 291-295.
920 Texler N. R., Holdway S., Neilson G. W. and Rode B. M. (1998) Monte Carlo
921 simulations and neutron diffraction studies of the peptide forming system 0.5 mol
922 kg^{-1} $CuCl_2$–5mol kg^{-1} NaCl–H_2O at 293 and 353 K. *J. Chem. Soc., Faraday Trans*.
923 **94**, 59-65.
924 Tsuchiya T., Abe M., Nakajima T. and Hirao K. (2001) Accurate relativistic Gaussian
925 basis sets for H through Lr determined by atomic self-consistent field calculations
926 with the third-order Douglas-Kroll approximation. *J. Chem. Phys.* **115**, 4463-4472.
927 van Duin A. C. T., Bryantsev V. S., Diallo M. S., Goddard W. A., Rahaman O., Doren
928 D. J., Raymand D. and Hermansson K. (2010) Development and validation of a
929 ReaxFF reactive force field for Cu cation/water interactions and copper metal/metal
930 oxide/metal hydroxide condensed phases. *J. Phys. Chem. A* **114**, 9507-9514.
931 van Rossum J. P. and Scharhart D. H. J. (1991) Oxidation-reduction (redox)
932 potentiometry in blood in geriatric conditions: a pilot study. *Exper. Gerontol.* **26**,
933 37-43.

934 Vance D., Archer C., Bermin J., Perkins J., Statham P. J., Lohan M. C., Ellwood M. J.
935 and Mills R. A. (2008) The copper isotope geochemistry of rivers and the oceans.
936 *Earth Planet. Sci. Lett*. **274**, 204-213.
937 Walker E. C., Cuttitta F. and Senftle F. E. (1958) Some natural variations in the relative
938 abundance of copper isotopes. *Geochim. Cosmochim. Acta* **15**, 183-194.
939 Weinstein C., Moynier F., Wang K., Paniello R., Foriel J. Catalano J. and Pichat S.
940 (2011) Isotopic fractionation of Cu in plants. *Chem. Geol*. **286**, 266-271.
941 Yoshio M., Ugamura M., Noguchi H. and Nagamatsu M. (1980) Applications of crown
942 ether in chemical analysis extraction of copper(II)-zincon chelate anion with crown
943 ether complex. *Anal. Lett*. **13**, 1431-1439.
944 Zhu X. K., O'Nions R. K., Guo Y., Belshaw N. S. and Rickard D. (2000) Determination
945 of Cu-isotope variation by plasma-source mass spectrometry: implications for use as
946 geochemical tracers. *Chem. Geol*. **163**, 139-149.
947 Zhu X. K., Guo Y., Williams R. J. P., O'Nions R. K., Matthews A., Belshaw N. S.,
948 Canters G. W., de Waal E. C., Weser U., Burgess B. K. and Salvato B. (2002) Mass
949 fractionation processes of transition metal isotopes. *Earth Planet. Sci. Lett*. **200**,
950 47-62.
951 Zirino A. and Yamamoto S (1972) A pH-dependent model for the chemical speciation
952 of copper zinc cadmium, and lead in seawater. *Limnol. Oceanogr*. **17**, 661-671.
953
954

Table 1 Isotopic fractionation of Cu(II) during exchange experiments between HCl medium and a macrocyclic complex.

[HCl] (M)	D	$\Delta^{65}Cu^{a}$ (‰)
1	1.3×10^{-4}	–1.06
2	1.8×10^{-3}	–0.84
3	2.4×10^{-2}	–0.77
4	1.5×10^{-1}	–0.65
5	4.6×10^{-1}	–0.61
6	9.8×10^{-1}	–0.39

[a] Errors are ±0.10‰ for 2σ.

Table 2 Nuclear field shift effect of Cu isotopes and isotopologues at 298 K.

Valence	Species	Total energy (a.u.)		ΔE (a.u.) (10^{-5})	Nuclear Field shift effect (‰)
		^{63}Cu	^{65}Cu		
Cu(0)	Cu^0	–1653.451898480	–1653.451827445	7.1035	–0.014
Cu(I)	Cu^+	–1653.210583752	–1653.210512731	7.1021	0.001
	CuCl	–2114.481787065	–2114.481716036	7.1029	–0.007
	CuH_2O^+	–1729.354508434	–1729.354437410	7.1024	–0.002
	CuOH	–1728.963440770	–1728.963369739	7.1031	–0.010
Cu(II)	Cu^{2+}	–1652.578696630	–1652.578625608	7.1022	0
	$CuCl^+$	–2114.155110496	–2114.155039471	7.1025	–0.003
	CuH_2O^{2+}	–1728.798913392	–1728.798842366	7.1026	–0.004
	$CuOH^+$	–1728.656622258	–1728.656551226	7.1032	–0.011
	CuO	–1728.336259331	–1728.336188299	7.1032	–0.011

[a] The nuclear field shift effect was calculated by $(\delta E_{\text{reference}} - \delta E_{\text{species}})/kT$ at T = 298K. The root-mean-square charge radii $\langle r^2\rangle^{1/2}$ reported for ^{63}Cu (3.8823×10^{-15} m) and ^{65}Cu (3.9022×10^{-15} m) (Angeli, 2004) were used. Cu^{2+} was set as the reference. Energy of photons of 1 a.u. is equal to 4.3597×10^{-18} J.

Table 3 Bond distances determined for $Cu(H_2O)_6^{2+}$.

$Cu\text{-}O_{ax}$ (Å)	$Cu\text{-}O_{eq}$ (Å)	Method[a]	Reference
2.30	2.02-2.03	MO	This study
2.25	2.06	MO	Beagley et al., 1989
2.25	2.05	MO	Åkesson et al., 1992
2.25	2.06-2.07	MO	Breza et al., 1997
2.23-2.26	2.033	MO	Bryantsev et al., 2008
2.46-2.58	1.97-2.09	MD	Liu et al., 2010
2.27	1.94	QM	van Duin et al., 2010
2.24	2.07	QM/MM MC	Marini et al., 1999
2.2-2.3	1.99-2.07	QM/MM MD	Schwenk and Rode, 2003a,b
2.60	1.955	EXAFS	Sham et al., 1981
2.28	2.00	EXAFS	Tajiri and Wakita, 1986
2.3	1.96	EXAFS	Nomura and Yamaguchi, 1988
2.29	1.99	EXAFS	Beagley et al., 1989
2.375-2.413	1.969-1.971	EXAFS	Fulton et al., 2000a,b
2.30	1.955	EXAFS	Persson et al., 2002
2.56	1.99	EXAFS+XANES	Benfatto et al., 2002
2.36	1.96	EXAFS+XANES	Chaboy et al., 2006
2.32	1.96	XANAS	Garcia et al., 1989
≥2.21	1.96	ND	Salmon et al, 1988
2.45	1.95	ND	Okan and Salmon, 1995
2.43	1.94	XRD	Ohtaki and Maeda, 1974
2.339	1.976	XRD	Magini, 1982

[a] MO (molecular orbital), EXAFS(extended x-ray absorption fine structure), MD (molecular dynamics), ND (neutron diffraction), QM(quantum mechanics), MM (molecular mechanics), MC (Monte Carlo), XANES (x-ray absorption near-edge structure), and XRD(x-ray diffraction).

Table 4 Bond distances determined for $Cu(H_2O)_5^{2+}$.

$Cu\text{-}O_{long}$ (Å)	$Cu\text{-}O_{short}$ (Å)	Method[a]	References
2.20	1.99-2.02	MO	This study
2.181	2.011	MO	Bryantsev et al., 2008
2.45	2.00	CPMD	Amira et al., 2005
2.22	2.04-2.07	CPMD	de Almeida et al., 2009
2.31	2.03-2.09	MD	Liu et al., 2010
2.34	1.963	EXAFS	Persson et al., 2002
2.39	1.97	EXAFS+XANES	Benfatto et al., 2002
2.36	1.96	EXAFS+XANES	Chaboy et al., 2006
–	1.96	ND	Pasquarello et al., 2001

[a] CPMD (Car-Parrinello MD)

Table 5 Logarithm of the reduced partition function, ln β, for the pair ^{65}Cu-^{63}Cu. Hydrated Cu(II) ions and chlorides.

Species	Temperature (K)					
	273	298	323	373	473	573
$Cu(H_2O)_5^{2+}$	5.355	4.546	3.905	2.968	1.876	1.290
$Cu(H_2O)_6^{2+}$	5.053	4.288	3.682	2.798	1.767	1.215
$CuCl(H_2O)_4^{+}$	4.906	4.161	3.572	2.712	1.711	1.176
$CuCl_2(H_2O)_3$	4.709	3.988	3.420	2.592	1.633	1.120
$CuCl_2(H_2O)_4$	4.397	3.724	3.193	2.421	1.525	1.046
$CuCl_3H_2O^{-}$	3.530	2.985	2.556	1.933	1.214	0.832

Table 6 Bond distances determined for $CuCl_m(H_2O)_n^{2-m}$.

Possible species	*m*	*n*	Cu-Cl[a] (Å)	Cu-O[a] (Å)	Method	References
$CuCl(H_2O)_4^+$	1	4	2.20	2.04-2.06(3) 2.35(1)	MO	This study
$CuCl(H_2O)_4^+$	1[b]	4	2.29[b]	1.968(3) 2.27(1)	EXAFS	D'Angelo et al., 1997
$CuCl(H_2O)_5^+$	1.1	5.2	2.55	2.00	MC	Rode and Islam, 1992
$CuCl_2(H_2O)_3$	2	3	2.25	2.07-2.08(2) 2.35(1)	MO	This study
$CuCl_2(H_2O)_3$	2.0	3.3	3.1	1.96	ND	Ansell et al, 1995
$CuCl_2(H_2O)_4$	2	4	2.27	2.11(2) 2.43(2)	MO	This study
$CuCl_2(H_2O)_4$	2	4	2.22	2.01(2) 2.28(2)	EXAFS	Tajiri and Wakita, 1986
$CuCl_2(H_2O)_4$	2.8	4.3	2.56	2.05(2) 2.5(2)	ND	Neilson, 1982
$CuCl_3H_2O^-$	3	1	2.22(1) 2.28(2)	2.28	MO	This study
$CuCl_3H_2O^-$	2.1	1	2.28	1.95	EXAFS	Collings et al., 2000
$CuCl_3(H_2O)_3^-$	3.3	2.7	2.43	1.90-1.95	XRD	Bell et al., 1973
$CuCl_4^{2-}$	3.8	0	2.24	–	EXAFS	Tanimizu et al., 2007
$CuCl_4(H_2O)_2^{2-}$	3.8	1.9	2.23	2.18	EXAFS	Tanimizu et al., 2007
$CuCl_4(H_2O)_2^{2-}$	4.2	2.3	2.56	2.05	ND	Neilson, 1982
$CuCl_4(H_2O)_2^{2-}$	3.6	2.4	2.43	1.90-1.95	XRD	Bell et al., 1973

[a] Number of bonds is shown in parentheses.
[b] An additional Cu-Cl bond distance of 2.85 Å reported may be too long to treat as chemical bonding.

Table 7 Logarithm of the reduced partition function, ln β, for the pair ^{65}Cu-^{63}Cu. Cu(II) hydroxides, carbonates, sulfate, and sulfides.

Species	Temperature (K)					
	273	298	323	373	473	573
$CuOH(H_2O)_4^+$	5.307	4.517	3.889	2.967	1.883	1.298
$Cu(OH)_2(H_2O)_3$	5.814	4.966	4.288	3.286	2.098	1.451
$CuCO_3(H_2O)_2$	5.091	4.323	3.715	2.825	1.787	1.230
$Cu(CO_3)_2^{2-}$	6.176	5.239	4.498	3.416	2.158	1.483
$CuHCO_3(OH)_2^-$	5.951	5.075	4.376	3.346	2.130	1.471
$CuSO_4(H_2O)_4$	6.041	5.144	4.430	3.381	2.148	1.481
$CuHS(H_2O)_4^+$	4.002	3.386	2.900	2.194	1.377	0.942
$Cu(HS)_2(H_2O)_3$	3.855	3.264	2.797	2.119	1.333	0.914

Table 8 Logarithm of the reduced partition function, ln β, for the pair ^{65}Cu-^{63}Cu. Hydrated Cu(I) ion, Cu(II) ascorbates, and Cu(II) oxalate.

Species	Temperature (K)					
	273	298	323	373	473	573
$Cu(H_2O)_2^+$, Cu(I)	3.368	2.867	2.468	1.882	1.193	0.822
$CuH(L\text{-ascorbate})(H_2O)_4^+$	3.924	3.324	2.850	2.161	1.362	0.935
$CuH(D\text{-ascorbate})(H_2O)_4^+$	3.989	3.380	2.899	2.199	1.386	0.951
$CuC_2O_4(H_2O)_2$	6.236	5.302	4.561	3.474	2.202	1.516

Figure captions

Figure 1 Mole fractions of Cu species and isotope fractionation of Cu in HCl solutions. a) Distribution of Cu chlorides. The mole fractions were calculated from the stability constants of Brugger (2001). b) Isotope fractionation is shown as $\Delta^{65}Cu = \delta^{65}Cu_{org} - \delta^{65}Cu_{aq}$ upon extraction of Cu by dicyclohexano-18-crown-6 (DC18C6) from the aqueous solution. The solid curves represent our estimates from the ln β values (298 K) of fivefold-coordinated $Cu(H_2O)_5^{2+}$, $CuCl(H_2O)_4^{2+}$, and $CuCl_2(H_2O)_3$, and $CuCl_3H_2O^-$ (Table 5), ln β_{CuLCl_2} (3.35‰), and *D*. The dotted curves represent the effect of ±0.05‰ errors on ln β_{CuLCl_2}.

Figure 2. Molecular structures of hydrated Cu^+, Cu^{2+}, and aqueous Cu(II) species. The structures are drawn using GaussView5 (Gaussian Inc.) (Dannington et al., 2009). Symbol keys: Cu (vermilion), Cl (green), S (yellow), O (red), C (gray), and H (white).

Figure 3. Temperature dependence of ln β. The ln β values of hydrated Cu^{2+} and Cu(II) chlorides (see Table 5) are shown as linear functions of T^{-2}.

Figure 4. Mole fractions of Cu(II) species and Cu isotopic variations as functions of pH at 298 K. a) Mole fractions of Cu species, b) Species $\delta^{65}Cu$ relative to the bulk solution. Literature values of formation constants at ionic strength I = 0.70 M (Powell et al., 2007) were used for the calculations. Σ[Cu(II)] was set to 10^{-9} M and it was assumed that the system was in equilibrium with air having a CO_2 fugacity of $10^{-3.5}$ bar (1 bar = 10^5 Pa) (Powell et al., 2007). We further assumed log $K[CO_2(g) = CO_2(aq)]$ = –1.5 (Morel and Hering, 1993) and concentrations of Cl^- = 0.55 mol kg^{-1} and SO_4^{2-} = 0.029 mol kg^{-1} (Macleod et al., 1994).

Figure 5. Temperature dependence of ln β. The ln β values of hydrated Cu(II) hydroxides, carbonates, sulfate, and sulfides (see Table 7) are shown as linear functions of T^{-2}.

Figure 6. Mole fractions of Cu(I) and Cu(II) species and Cu isotopic variations as functions of Eh and extent of oxalate formation at 298 K. pH and total Cu concentration were set to be 7.4 and 1 μM, respectively a) Mole fractions of Cu species as functions of Eh. Concentrations of ascorbate and oxalate were set to 90 μM and 10 μM, respectively. b) Mole fractions of Cu species as functions of proportion of oxalate formed. Eh was set to be 0.27 V. c) δ^{65}Cu relative to the bulk solution as functions of Eh. Conditions are identical to those of a, and d) δ^{65}Cu relative to the bulk solution as functions of extent of oxalate formation. Conditions are identical to those of b.

Figure 7. Temperature dependence of ln β. The ln β values of hydrated Cu^{+} and Cu(II) oxalate and ascorbate (see Table 8) are shown as linear functions of T^{-2}. The ln β values of pentaaqua Cu^{2+} (see Table 5 and Fig. 3) are shown together.

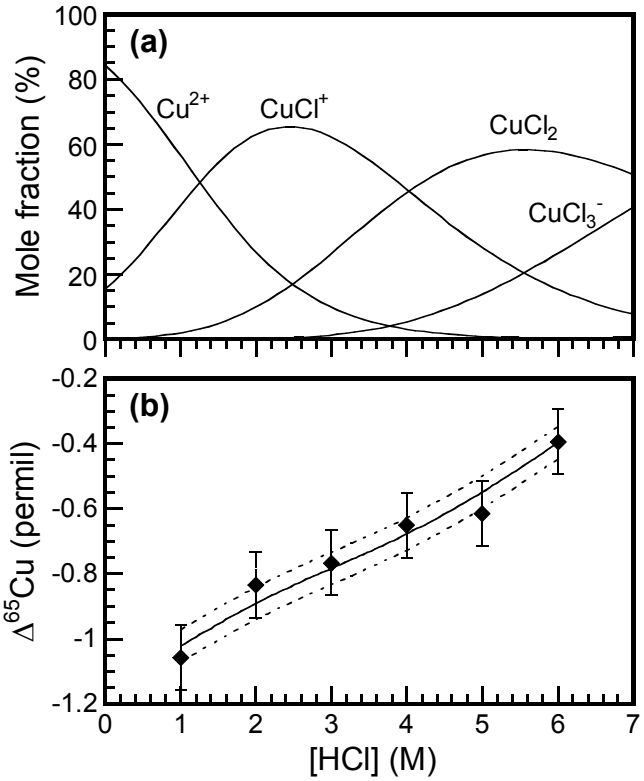
(a)
Mole fraction (%)
100
80
60
40
20
0
Cu2+
CuCl+
CuCl2
CuCl3-
(b)
Δ65Cu (permil)
-0.2
-0.4
-0.6
-0.8
-1
-1.2
0
1
2
3
4
5
6
7
[HCl] (M)

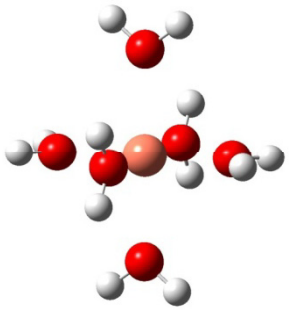

a) $Cu(H_2O)_6^{2+}$

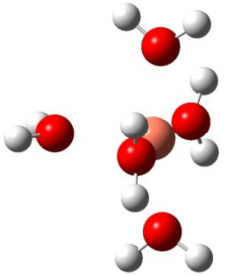

b) $Cu(H_2O)_5^{2+}$

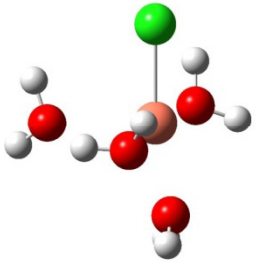

c) $CuCl(H_2O)_4^{+}$

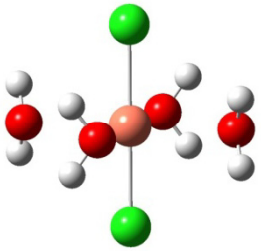

d) $CuCl_2(H_2O)_4$

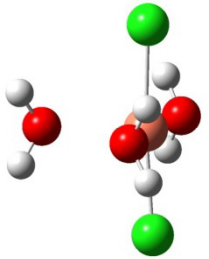

e) $CuCl_2(H_2O)_3$

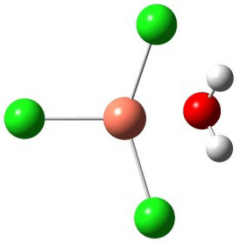

f) $CuCl_3H_2O^{-}$

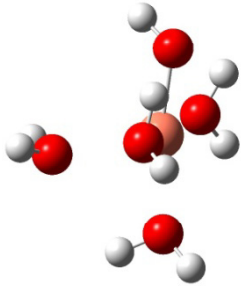

g) $CuOH(H_2O)_4^{-}$

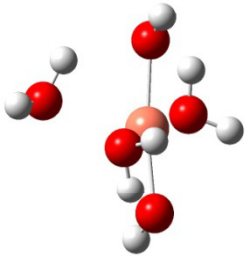

h) $Cu(OH)_2(H_2O)_3$

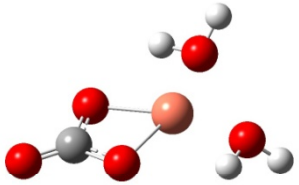

i) $CuCO_3(H_2O)_2$

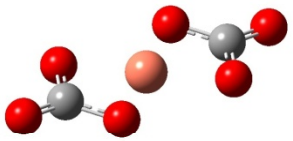

j) $Cu(CO_3)_2^{2-}$

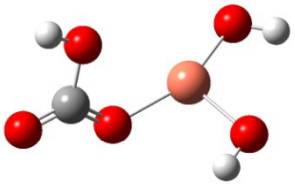

k) $CuHCO_3(OH)_2^{-}$

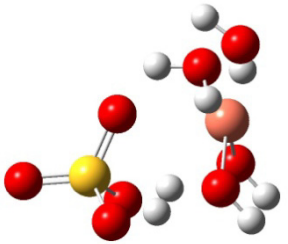

l) $CuSO_4(H_2O)_4$

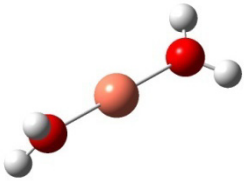

m) $Cu(H_2O)_2^{+}$, Cu(I)

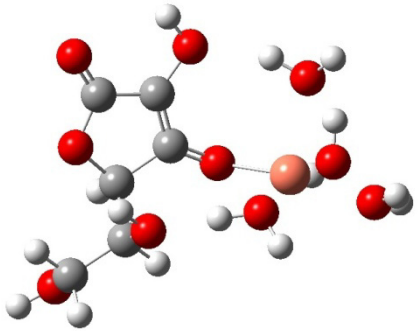

n) $CuHA(H_2O)_4^{+}$
(A: L-ascorbate)

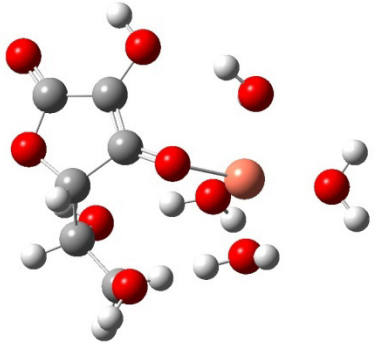

o) $CuHA(H_2O)_4^{+}$
(A: D-ascorbate)

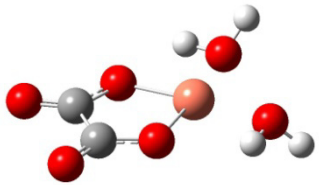

p) $CuC_2O_4(H_2O)_2$

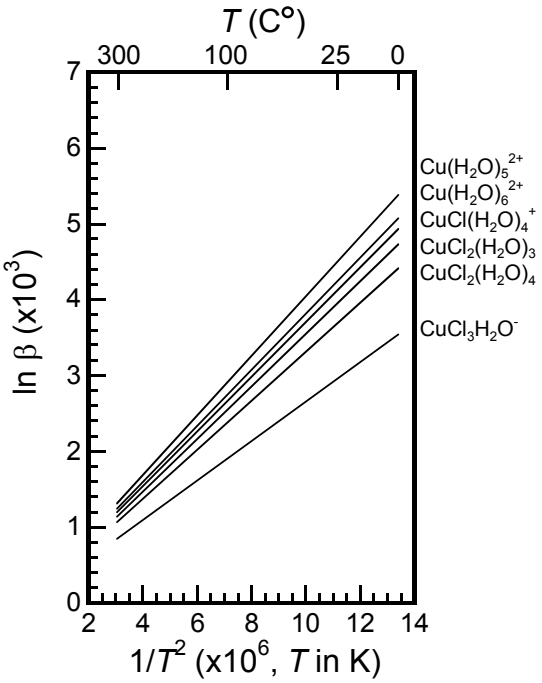
T (C°)
300
100
25
0
7
6
5
4
3
2
1
0
ln β (x10^3)
2
4
6
8
10
12
14
1/T^2 (x10^6, T in K)
Cu(H2O)5 2+
Cu(H2O)6 2+
CuCl(H2O)4 +
CuCl2(H2O)3
CuCl2(H2O)4
CuCl3H2O-

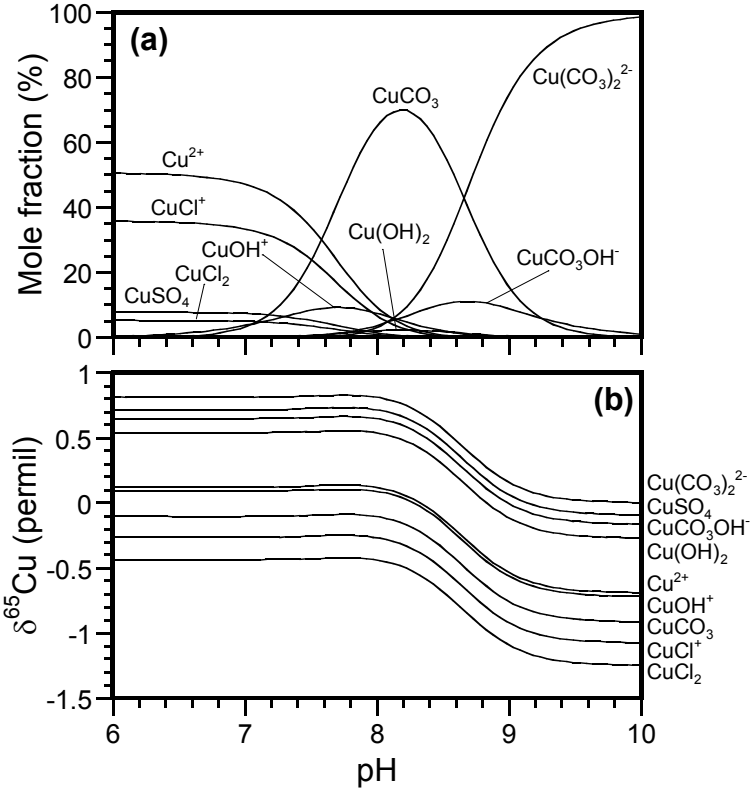
(a)
Mole fraction (%)
100
80
60
40
20
0
Cu2+
CuCl+
CuOH+
CuCl2
CuSO4
CuCO3
Cu(OH)2
Cu(CO3)2 2-
CuCO3OH-
(b)
δ65Cu (permil)
1
0.5
0
-0.5
-1
-1.5
Cu(CO3)2 2-
CuSO4
CuCO3OH-
Cu(OH)2
Cu2+
CuOH+
CuCO3
CuCl+
CuCl2
6
7
8
9
10
pH

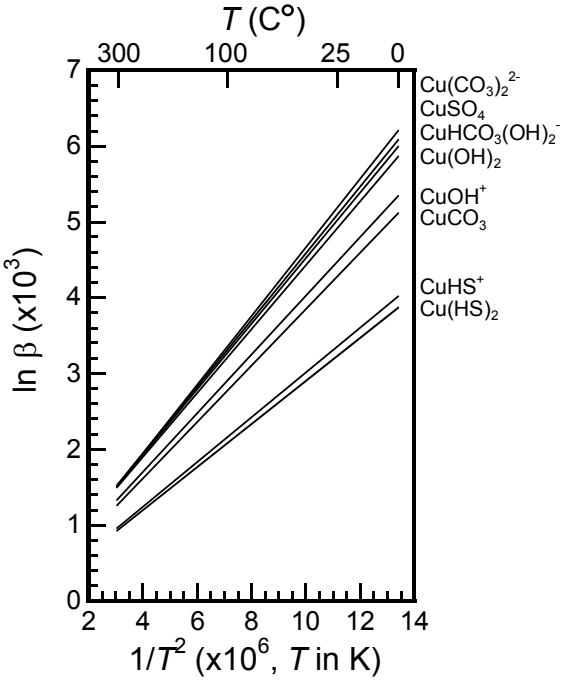
T (C°)
300
100
25
0
7
6
5
4
3
2
1
0
ln β (x10^3)
2
4
6
8
10
12
14
1/T^2 (x10^6, T in K)
Cu(CO3)2 2-
CuSO4
CuHCO3(OH)2 -
Cu(OH)2
CuOH+
CuCO3
CuHS+
Cu(HS)2

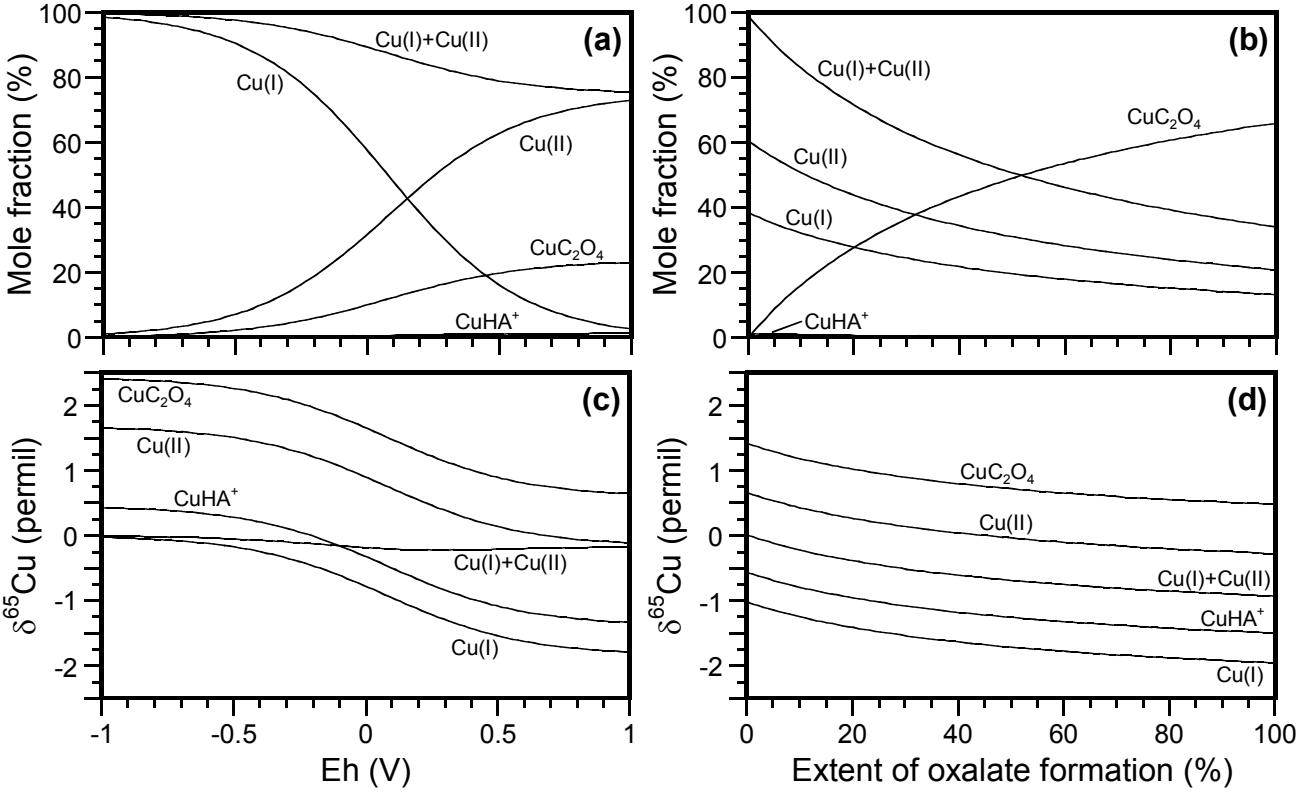
(a)
(b)
(c)
(d)
Mole fraction (%)
Cu(I)+Cu(II)
Cu(I)
Cu(II)
CuC_2O_4
$CuHA^+$
δ^{65}Cu (permil)
Eh (V)
Extent of oxalate formation (%)

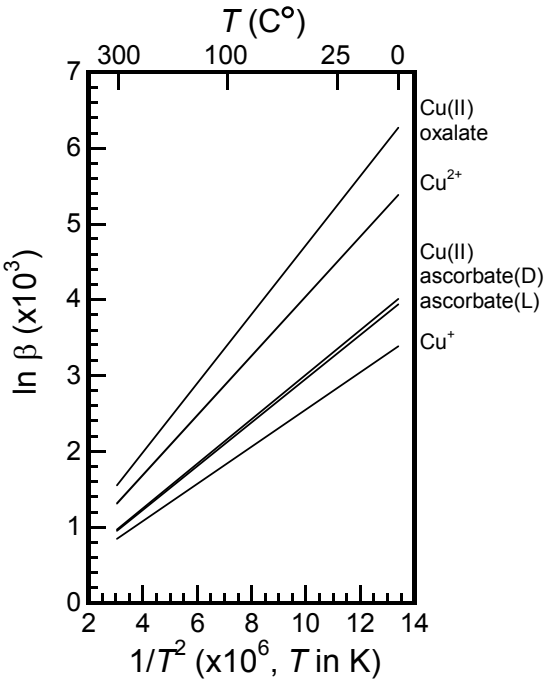
T (C°)
300
100
25
0
7
6
5
4
3
2
1
0
ln β (x10^3)
2
4
6
8
10
12
14
1/T^2 (x10^6, T in K)
Cu(II)
oxalate
Cu2+
Cu(II)
ascorbate(D)
ascorbate(L)
Cu+

Supporting Information

Copper isotope fractionation between aqueous compounds relevant to low temperature geochemistry and biology

Toshiyuki Fujii[1]*, Frédéric Moynier[2], Minori Abe[3],
Keisuke Nemoto[3], and Francis Albarède[4]

[1] Research Reactor Institute, Kyoto University, 2-1010 Asashiro Nishi, Kumatori, Sennan, Osaka 590-0494, Japan

[2] Department of Earth and Planetary Sciences and McDonnell Center for Space Sciences, Washington University in St. Louis, Campus Box 1169, 1 Brookings Drive, Saint Louis, MO 63130-4862, USA

[3] Department of Chemistry, Graduate School of Science and Engineering, Tokyo Metropolitan University, 1-1 Minami-Osawa, Hachioji-shi, Tokyo 192-0397, Japan

[4] Ecole Normale Supérieure de Lyon, Université de Lyon 1, CNRS, 46, Allee d'Italie, 69364 Lyon Cedex 7, France

Table S1. Optimized structure Cartesian coordinates of hydrated Cu(I) and Cu(II) ions and Cu(II) complexes. (see Figure 2).

$Cu(H_2O)_5^{2+}$

Element	X	Y	Z
Cu	0.000000	0.000000	0.180286
O	-0.000218	1.972347	0.416359
O	-2.015695	0.000003	0.367094
O	0.000218	-1.972347	0.416359
O	2.015695	-0.000003	0.367094
O	0.000000	0.000000	-2.017628
H	-0.788497	2.520100	0.544468
H	0.787668	2.520277	0.546113
H	-0.787668	-2.520277	0.546113
H	0.788497	-2.520100	0.544468
H	-2.541191	0.000171	1.181710
H	-2.620652	-0.000935	-0.390193
H	2.541191	-0.000171	1.181710
H	2.620652	0.000935	-0.390193
H	-0.000087	0.774145	-2.598417
H	0.000087	-0.774145	-2.598417

$Cu(H_2O)_6^{2+}$

Element	X	Y	Z
Cu	0.000038	-0.000034	0.000063
O	-0.088873	2.019575	0.031113
O	-0.024969	-0.086591	2.300836
O	2.025399	0.080251	0.024068
O	0.088810	-2.019630	-0.031022
O	0.024925	0.086561	-2.300618
O	-2.025376	-0.080204	-0.023865
H	0.668784	2.613652	0.123299
H	-0.902057	2.538568	0.101414
H	0.902001	-2.538615	-0.101323
H	-0.668838	-2.613716	-0.123240
H	-0.067738	0.644710	2.931884
H	0.005459	-0.892336	2.834501
H	-0.005323	0.892306	-2.834292
H	0.067755	-0.644755	-2.931647
H	2.576945	0.077097	0.819263
H	2.591990	0.154602	-0.756953
H	-2.591929	-0.154550	0.757185
H	-2.576976	-0.076949	-0.819023

$CuCl(H_2O)_4^{2+}$

Element	X	Y	Z
Cu	-0.016654	0.212129	-0.176174
Cl	-0.368293	-1.902143	-0.655033
O	-0.263347	-0.047793	1.850095
O	2.209959	-0.237365	0.440996
O	-0.036021	2.218349	0.250375
O	-0.057535	0.711653	-2.157294
H	0.598254	-0.331813	2.193790
H	-0.889110	-0.757015	2.061119
H	0.438028	2.925105	-0.204498
H	-0.248494	2.513422	1.145250
H	3.038932	0.256513	0.412129
H	2.414530	-1.133283	0.138808
H	-0.785481	1.250808	-2.496952
H	-0.059913	-0.113878	-2.668013

$CuCl_2(H_2O)_3$

Element	X	Y	Z
Cu	-0.053962	0.000888	-0.169852
Cl	0.052761	2.249760	-0.117204
Cl	0.050030	-2.247826	-0.115168
O	-0.166668	0.001703	1.905225
O	0.472730	-0.000037	-2.167140

O	-2.337733	0.004542	-0.702549
H	0.114046	0.787034	-2.597917
H	0.111330	-0.785773	-2.598069
H	0.267547	-0.788948	2.253624
H	0.269249	0.791416	2.253590
H	-2.746356	0.783330	-0.306552
H	-2.752723	-0.768865	-0.302717

$CuCl_2(H_2O)_4$

Element	X	Y	Z
Cu	0.000113	-0.000205	0.000036
Cl	0.001187	-2.268694	0.000102
Cl	-0.000962	2.268241	-0.000026
O	0.417498	0.000178	2.071588
O	2.327682	0.000039	-0.692256
O	-0.417251	-0.000257	-2.071517
O	-2.327453	-0.001831	0.692327
H	-2.708483	-0.776704	0.262520
H	-2.710171	0.772049	0.262246
H	0.031352	0.780962	-2.422591
H	0.032951	-0.780315	-2.423107
H	2.709142	-0.774664	-0.262522
H	2.709964	0.774089	-0.262095
H	-0.031968	0.780871	2.422726
H	-0.031827	-0.780407	2.423132

$CuCl_3H_2O^-$

Element	X	Y	Z
Cu	0.009270	0.089718	-0.002037
Cl	2.197046	0.600440	0.407279
Cl	-0.053553	-0.775059	-2.050390
Cl	-2.075181	0.930696	0.398702
O	-0.031900	-0.399468	2.220232
H	-0.770277	0.213170	2.362199
H	0.792853	0.090825	2.362505

$CuOH(H_2O)_4^+$

Element	X	Y	Z
Cu	-0.022412	-0.011572	0.135042
O	2.055857	0.070828	-0.052489
O	-2.050422	0.169765	-0.181485
O	0.159947	1.789601	-0.261094
O	-0.205225	-2.061829	0.224458
O	0.053073	-0.361275	2.421138
H	2.051118	1.010485	-0.319345
H	2.660380	-0.414596	-0.627116
H	-2.204931	0.986925	-0.676734

H	-2.650954	-0.512055	-0.507452
H	-0.097467	2.412135	0.429233
H	-0.047966	-2.399730	1.116909
H	0.091646	-2.725054	-0.410229
H	0.872675	-0.124189	2.873930
H	-0.665321	-0.109440	3.015233

$Cu(OH)_2(H_2O)_3$

Element	X	Y	Z
Cu	-0.258245	-0.086613	-0.062472
O	-0.074679	-0.232907	1.820662
O	2.081764	0.067472	0.259624
O	-0.399476	2.106958	-0.460200
O	-0.677539	0.056454	-1.875154
O	-0.551081	-2.201797	0.273191
H	-0.175399	-0.497968	-2.477903
H	-1.413113	-2.553797	0.027322
H	-0.566410	-1.987168	1.228999
H	2.369866	0.976539	0.124900
H	1.738922	0.025664	1.174903
H	-1.195357	2.594308	-0.223017
H	-0.543869	1.724067	-1.363498
H	-0.468696	0.448284	2.370949

$CuCO_3(H_2O)_2$

Element	X	Y	Z
Cu	0.248982	0.000870	-0.001777
O	1.470106	1.668045	-0.237640
O	1.470728	-1.665996	0.239991
O	-1.340955	1.081270	-0.128922
O	-1.338478	-1.082522	0.125223
O	-3.325503	-0.003074	-0.002008
C	-2.117328	-0.001419	-0.001917
H	2.092931	1.971316	0.432853
H	0.791443	2.353819	-0.329161
H	0.791117	-2.351065	0.329900
H	2.096954	-1.971245	-0.426543

$Cu(CO_3)_2^{2-}$

Element	X	Y	Z
Cu	0.000000	0.000000	0.000000
O	1.670093	1.094791	0.000000
O	1.670093	-1.094791	0.000000
O	-1.670093	1.094791	0.000000
O	-1.670093	-1.094791	0.000000
O	3.658669	0.000000	0.000000
O	-3.658669	0.000000	0.000000

C	2.413378	0.000000	0.000000
C	-2.413378	0.000000	0.000000

$CuHCO_3(OH)_2^-$

Element	X	Y	Z
Cu	0.328828	-0.274402	0.333280
O	-0.217938	0.652837	1.889544
O	2.152371	-0.434121	0.505155
O	-1.358315	-0.720389	-0.512057
O	-2.850925	-0.477652	-2.183668
O	-0.850477	0.562886	-2.262179
C	-1.778817	-0.270627	-1.625885
H	2.446380	-0.021985	1.321861
H	-1.181615	0.642755	1.857756
H	-1.280353	0.840660	-3.079424

$CuSO_4(H_2O)_4$

Element	X	Y	Z
Cu	0.747523	-0.018631	0.075914
S	-2.464712	0.089386	0.319198
O	0.888308	1.472448	-1.374296
O	1.260468	-1.547098	-1.216183
O	-1.460921	0.074115	-0.784172
O	-3.860376	0.146652	-0.015297
O	-2.105782	1.314366	1.248990
O	-2.198978	-1.199463	1.194935
O	0.426005	1.463763	1.245656
O	0.334120	-1.521773	1.204522
H	0.822684	1.412610	2.120663
H	0.727408	-1.537786	2.082364
H	-1.070215	1.435319	1.324962
H	-1.181852	-1.395474	1.269655
H	-0.031570	1.461652	-1.687718
H	0.699514	-1.631741	-1.997308
H	0.934346	2.226004	-0.763219
H	0.994031	-2.244346	-0.588664

$CuHS(H_2O)_4^+$

Element	X	Y	Z
Cu	0.005656	0.054181	0.049629
S	0.046759	2.225860	-0.652513
O	2.066189	0.034639	0.017085
O	-2.046642	0.067176	-0.000969
O	-0.098475	-2.084607	0.119384
O	-0.014729	-0.342819	2.333240
H	2.342733	0.886375	-0.359080
H	2.619756	-0.660348	-0.362321

H	-2.350685	0.888640	-0.417416
H	-2.561894	-0.668691	-0.356925
H	0.013829	2.775894	0.581471
H	-0.038801	-2.444466	1.013933
H	0.055219	-2.798994	-0.509691
H	0.752827	-0.111541	2.871191
H	-0.791745	-0.101300	2.852979

$Cu(HS)_2(H_2O)_3$

Element	X	Y	Z
Cu	-0.314974	-0.153083	0.141975
S	-0.177791	-0.026204	2.425827
S	-0.977088	-0.352010	-2.086603
O	2.022133	0.047647	0.018214
O	-0.359897	2.013095	-0.277947
O	-0.584294	-2.264904	0.309083
H	0.260936	-0.547023	-2.586321
H	-1.025393	-2.457587	-0.533692
H	-1.180639	-2.509597	1.028124
H	2.206699	0.965967	-0.211249
H	2.078845	0.012600	0.986178
H	-1.007256	2.546627	0.198468
H	-0.707717	1.864863	-1.179080
H	-0.366876	1.299105	2.585329

$Cu(H_2O)_2^+$, Cu(I)

Element	X	Y	Z
Cu	0.000000	0.000000	0.000000
O	1.917316	0.000000	0.000000
O	-1.917316	0.000000	0.000000
H	2.479474	0.000000	0.785072
H	2.479474	0.000000	-0.785072
H	-2.479474	0.785072	0.000000
H	-2.479474	-0.785072	0.000000

$CuH(\text{L-ascorbate})(H_2O)_4^+$

Element	X	Y	Z
Cu	-2.554119	0.204618	-0.182677
O	2.495659	-1.159318	2.512367
O	2.452051	-0.123655	0.482443
O	0.832979	2.264059	0.187868
O	2.921441	1.402529	-2.662114
O	-0.251520	-1.875139	2.006688
O	-0.902877	-0.653920	-0.701190
O	-1.802772	1.980765	0.480774
O	-2.984382	-1.344893	1.462135
O	-3.638265	-1.258716	-1.373516

O	-4.488981	1.096700	-0.188664
C	0.210170	-0.634730	-0.055714
C	0.533793	-1.180051	1.159370
C	1.917511	-0.858682	1.501999
C	1.476723	0.028661	-0.581649
C	1.324332	1.507831	-0.932285
C	2.611406	2.124521	-1.479680
H	0.282491	-2.124993	2.781107
H	1.856949	-0.495139	-1.462939
H	0.550722	1.582431	-1.699857
H	2.426476	3.184812	-1.685448
H	3.412119	2.041566	-0.733982
H	1.495728	2.278551	0.891165
H	3.769228	1.694906	-3.011156
H	-0.822376	2.131725	0.453305
H	-2.229187	2.799140	0.202579
H	-5.124762	0.619254	-0.737069
H	-4.976734	1.533791	0.518984
H	-2.135960	-1.697050	1.787704
H	-3.557018	-1.253973	2.232088
H	-3.692109	-2.023413	-0.782479
H	-3.169074	-1.562546	-2.161632

CuH(D-ascorbate)$(H_2O)_4^+$

Element	X	Y	Z
Cu	1.338456	0.278439	2.323761
O	0.071296	1.001644	1.087992
O	3.072810	0.897735	1.231687
O	1.773378	-1.729001	1.305373
O	-0.285916	0.071930	3.660925
O	2.706954	0.025220	3.885105
O	1.836297	1.689085	-1.258622
O	0.437176	0.641637	-3.585234
O	-1.131435	-0.102936	-2.109935
O	-0.309048	-2.292050	-0.476613
O	-2.377214	-0.591814	1.927738
C	-0.098546	0.703108	-0.149174
C	0.661040	1.030157	-1.240427
C	0.029557	0.534435	-2.460046
C	-1.310506	-0.058681	-0.671084
C	-1.489555	-1.515966	-0.211950
C	-1.770799	-1.723141	1.289766
H	-2.225667	0.499580	-0.459825
H	-2.314597	-1.919188	-0.807171
H	-0.261507	-2.495742	-1.418672
H	-2.380007	-2.618680	1.425075
H	-0.818875	-1.901148	1.791013

H	-3.309482	-0.757823	2.100138
H	2.102750	1.825492	-2.183748
H	2.843084	1.455503	0.467547
H	3.464206	0.098983	0.853094
H	3.521725	0.542562	3.868942
H	2.519606	-0.218994	4.798761
H	-1.112200	0.003512	3.130698
H	-0.438922	0.769088	4.309435
H	1.151785	-2.028910	0.608694
H	2.088039	-2.518759	1.759410

$CuC_2O_4(H_2O)_2$

Element	X	Y	Z
Cu	0.220299	0.001436	-0.001762
O	-1.136604	0.668638	1.127124
O	-1.137806	-0.672486	-1.125207
O	-3.370391	0.723223	1.234860
O	-3.371751	-0.739772	-1.222759
O	1.501827	0.874109	1.359112
O	1.503177	-0.864008	-1.365652
C	-2.354928	0.396973	0.678715
C	-2.355545	-0.407526	-0.671427
H	0.833390	1.221592	1.973878
H	2.155906	0.391795	1.877813
H	2.155176	-0.378487	-1.884016
H	0.837250	-1.215488	-1.980679

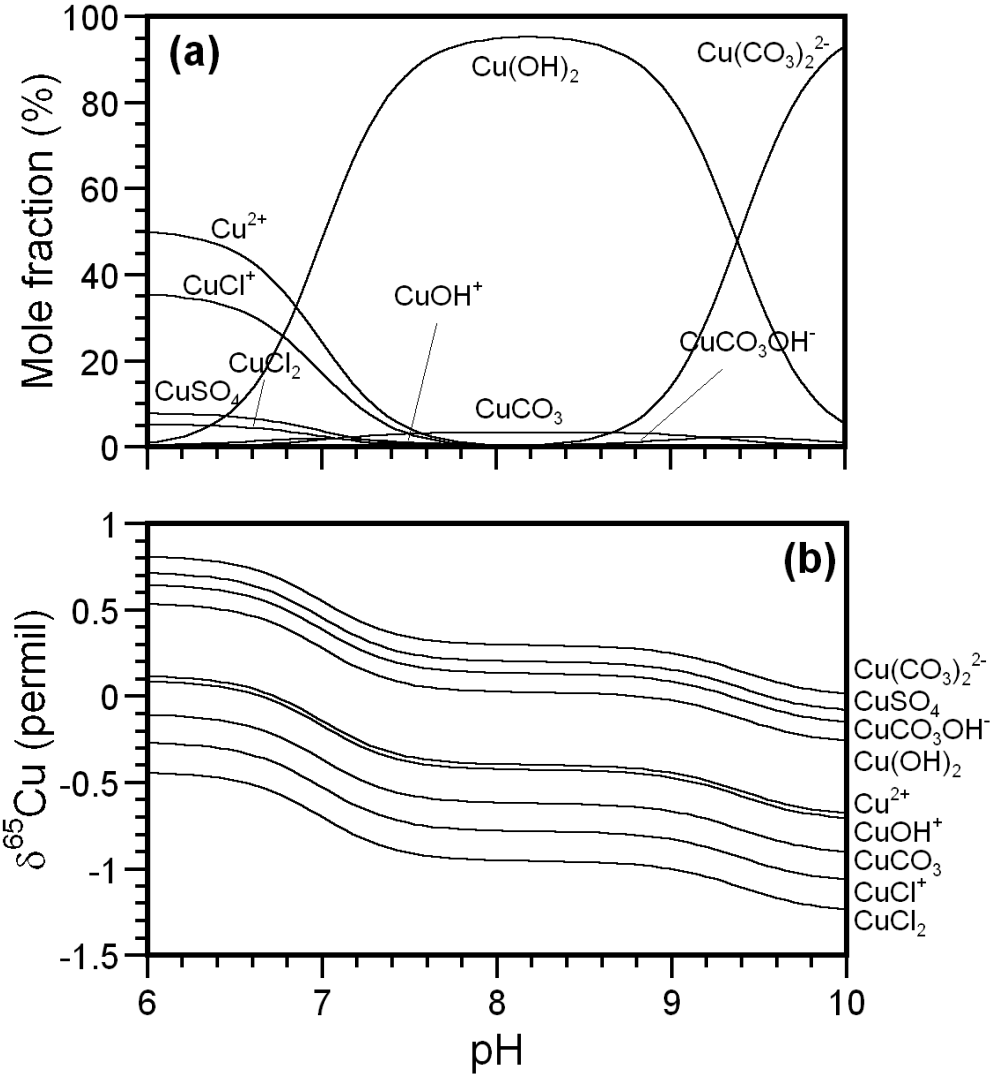

Figure S1. Mole fractions of Cu(II) species and Cu isotopic variations as functions of pH at 298 K. a) Mole fractions of Cu species, b) Species δ^{65}Cu relative to the bulk solution. Conditions are the same with those of Fig. 4 except for second hydrolysis constant. log*β_2 = –16.65 used in Fig. 4 was substituted by log β_2 = 14.3 and ion product pK_W = 14 (ionic strength I = 0).